First Tomographic Imaging of Mid-Crustal Doubling at the Abruzzi Outer Thrust Front, Central-Southern Italy

Rita de Nardis[1,2], Donato Talone[1,2], Luca De Siena[2,3], Maria Adelaide Romano[4], Francesco Brozzetti[1,2], Giusy Lavecchia[1,2]

[1]Department of Sciences, Study University "G. d'Annunzio" Chieti – Pescara, Chieti, 66013, Italy
[2]CRUST – Interuniversity Centre for 3D Seismotectonics with Territorial Applications, Chieti, 66013, Italy
[3]Department of Physics and Astronomy (DIFA), Alma Mater Studiorum University of Bologna, Bologna, 40127, Italy
[4]National Institute of Oceanography and Applied Geophysics – OGS, Trieste, 34010, Italy

Correspondence to: Rita de Nardis (rita.denardis@unich.it) and Donato Talone (donato.talone@unich.it)

Abstract. The geometry, deep structural style, and seismotectonic setting of the outer Abruzzi thrust system are less understood than those of other segments of Italy's Late Pliocene–Quaternary contractional belt. This knowledge gap arises from the region's complex surface geology, low seismicity rates, and the limited resolution of existing geophysical data.

Here, we present a local earthquake tomography of a large and previously unexplored area that encompasses the Abruzzi thrust system and spans from the Apennine extensional province in the west to the foreland strike-slip province in the east. The model is based on the inversion of 42,176 P-wave and 29,045 S-wave arrival times from earthquakes with M_L ranging from 0.2 to 5.5.

Our results show low seismic velocities at upper crustal levels in the western sectors, correlating with continental basins of the extensional domain. In contrast, marked Vp inversions (decrease in velocity with depth) at mid- to lower-crustal depths in the eastern sector delineate a crustal doubling.

We interpret the tomographic results in the context of geological, geophysical, and seismological data to construct a 3D conceptual model of the region. This includes the ~~first~~ geometric reconstruction of the Abruzzi Arc basal thrust, an eastward convex arcuate structure extending ~170 km and reaching depths of ~ 24 km. The model also incorporates strike-slip faults in the footwall and east-dipping normal faults to the west.

The structural affinity between the Abruzzi Arc basal thrust and other seismogenic structures of the Padan–Adriatic belt, located in the same structural position, suggests potential seismogenic behavior, although slow deformation rates and long recurrence intervals obscure its seismic expression. This conceptual model provides new insights into regional geodynamics and has significant implications for seismic hazard assessment in the central–southern Apennine transition zone.

1 Introduction

Characterizing the deep geometry and the deformation style of large compressive structures is essential for understanding their roles in the regional stress field, assessing seismic hazards, and refining geodynamic models. Classifying tectonic structures as thick- or thin-skinned is valuable for building reliable tectonic models and better defining the arrangement and behaviour of faults, which control the occurrence, magnitude, and type of earthquakes.

Building such models is especially challenging in zones with slow deformation and complex crustal settings. In these areas, earthquake occurrence may seem erratic and episodic, with events sparsely distributed (e.g., fault creep), or absent (e.g., locked or inactive fault). As a result, tectonic structures loading at slow rates may be seen as either active, associated with long-period recurrent earthquakes (Lu et al., 2020; Mazzotti et al., 2020; Ramalho et al., 2022), or inactive.

This dichotomy characterizes many seismogenic regions worldwide, such as the Eastern Betics (e.g., Gómez-Novell et al., 2020; Martín-Banda et al., 2021), Western Iberia (e.g., Custódio et al., 2015; Matos et al., 2018), Southern Mongolia (e.g., Bollinger et al., 2021; Van Der Wal et al., 2021), southwestern China (~~near~~ e.g., the Longmen Shan fault, the source of the M7.9 earthquake that struck Sichuan Province in 2008) (e.g., Kirby et al., 2008; Zhang et al., 2009), and the High Atlas zone, where a M_W 6.8 earthquake occurred unexpectedly in 2023 (e.g., Cheloni et al., 2024; Yeck et al., 2023).

This ambiguity leads to significant uncertainties when characterizing seismicity, tectonic features, and seismic hazards. In areas with low deformation, the seismogenic potential of faults can be difficult to determine. This is especially true for buried thrust structures along the coast or offshore, where direct measurements like paleoseismological studies or GPS estimates are often not feasible or available.

The contractional seismotectonic province of Italy (Lavecchia et al., 2021b) is a clear example of a slowly deforming zone (Carafa and Bird, 2016; Petricca et al., 2019). The activity and deformation style of the Outer Thrust System (OTS) of the Apennine-Maghrebian fold-and-thrust belt, extending thousands of kilometres along strike from northern Italy to Sicily (Figs. 1a, S1), have long puzzled scientists (Lavecchia et al., 2007; Mazzoli et al., 2000; Petricca et al., 2019; Scrocca et al., 2005; Vannoli et al., 2015; Visini et al., 2010). GPS data indicate a convergence rate of 1-3 mm/yr (Devoti et al., 2017) (Figs. 1b, 1c). This velocity varies along the OTS and, besides the coastal and offshore regions, does not fully capture the current deformation (Carafa and Bird, 2016). Recently, Pezzo et al. (2020), through targeted experiments, measured the convergence rates using GNSS stations installed on platforms in the northern Adriatic offshore. Borehole breakout and focal mechanisms (Mariucci and Montone, 2022) highlight an active contractional zone, characterized mainly by sub-horizontal P-axes, striking nearly SSW-NNE along the Padan Arc in the northern Apennines, WSW-ENE along the Adriatic Arc, and approximately S-N in Sicily (Figs. 1a, b, S1). There is a lack of seismogenic compression along the OTS front in southern Italy. Generally, the contractional zone shows low background seismicity, with historic and instrumental earthquakes rarely exceeding M_W 6.0 (CPTI15.v4, DISS Working Group, 2021; Petricca et al., 2019; Rovida et al., 2020).

This paper focuses on the Abruzzi Arc basal thrust in the transition zone between the Central and Southern Apennines, south of the Adriatic Arc (Figs. 1b, 2, 3a, 3b, S1). Its architecture, crustal structure, and seismotectonic role have not been fully defined.

Although local evidence suggests active thrusting through topographic relief and fluvial network analyses (Ferrarini et al., 2021a), the crustal geometry remains debated despite numerous studies (Butler et al., 2004; Calabrò et al., 2003; D'Ambrosio et al., 2021; Lacombe and Bellahsen, 2016; Mostardini and Merlini, 1986), which include deep crust seismic reflection data (e.g., CROP11, Di Luzio et al., 2009; Patacca et al., 2008). Moreover, previous tomographic images barely cover the study

area (41.00°- 42.50° latitude and 12.60°-15.60° longitude), or they are located north or south of it (Chiarabba et al., 2010; Improta et al., 2014; Zhao et al., 2016).

The seismic quiescence of the Abruzzi Arc basal thrust during the instrumental period raises unresolved questions about seismic hazard and geodynamics of this area (e.g., Lanari et al., 2023; Pace et al., 2006). Is it an inactive segment of the Italian OTS or a potentially locked fault?

Uncertainty mainly arises from the unclear connection between thrust faults and historic earthquakes. The macroseismic epicentres of some destructive events align with the boundaries of the contractional zone (Figs. 2a and Fig. S2). Thus, they could be associated either with the Abruzzi Arc basal thrust or with the adjacent seismotectonic domains, i.e., the extensional Apennine province to the west and the strike-slip foreland province to the east (Figs. 2, S2).

From a geodynamic perspective, the substantial difference in compressive seismic activity between the northern seismic Padan-Adriatic Arc and the prevailingly aseismic southern Apennines, including the Abruzzi Arc basal thrust, has led to various interpretations, mainly linked to a different along-strike configuration of the Adriatic slab. Possible explanations include slab rollback (Wortel and Spakman, 2000), asthenospheric upwelling (Cimini and De Gori, 2001), petrological variations in the slab (Giacomuzzi et al., 2022), or even the absence of the Adriatic subduction (Bell et al., 2013; Lavecchia and Creati, 2006).

To gain insights into this conundrum, we 1) perform a novel local earthquake tomography that provides 3D P and S velocity models, delineating the main features of subsurface tectonic setting; 2) revise microseismicity calculating new focal mechanisms; 3) collect and review geological and geophysical data from the available literature; 4) provide the conceptual 3D reconstruction of the Abruzzi Arc basal thrust integrating it into a broader tectonic framework that includes both the neighbouring extensional and strike-slip seismogenic structures.

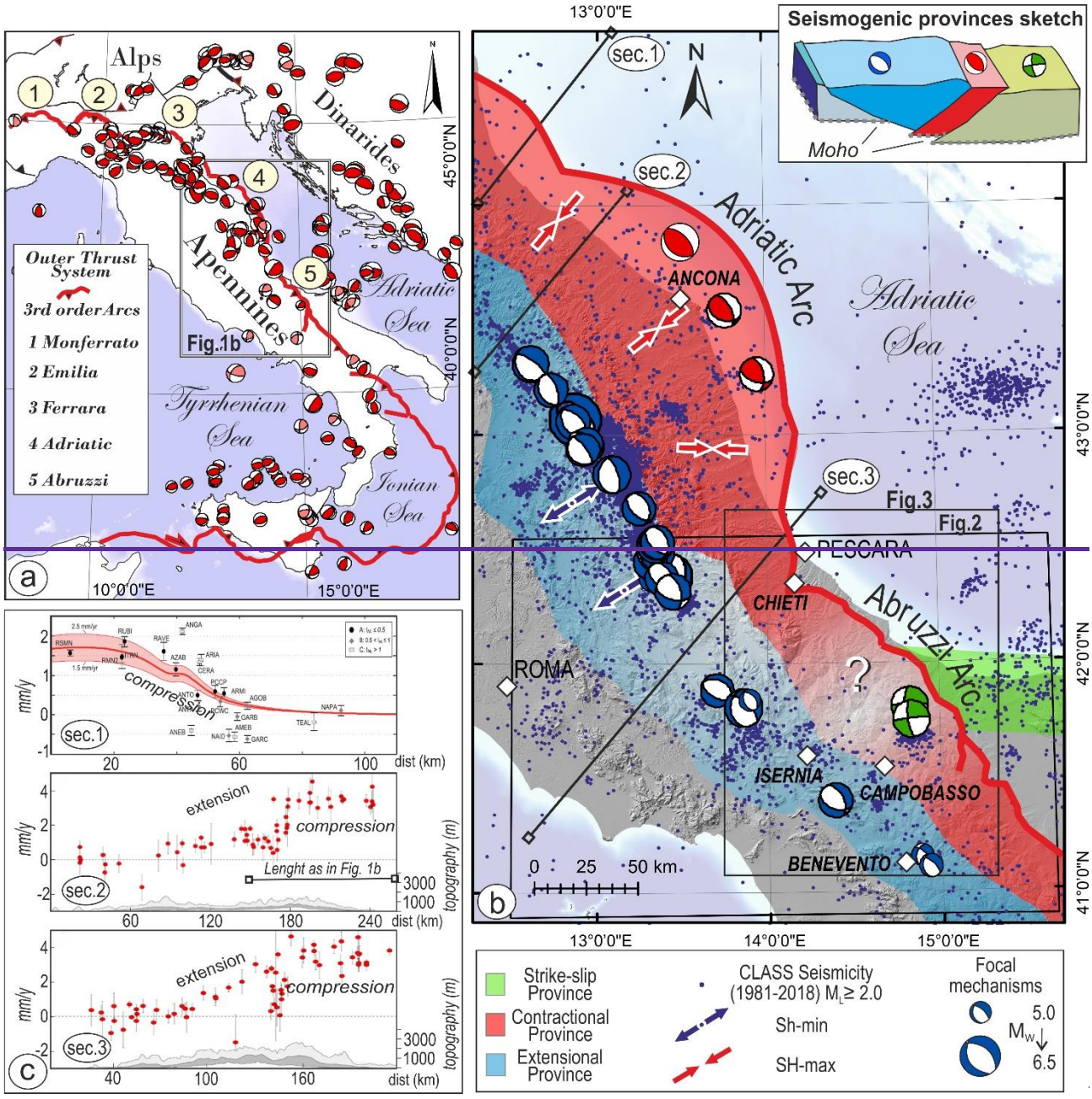
Alps
Dinarides
Apennines
Adriatic Sea
Tyrrhenian Sea
Ionian Sea
Outer Thrust System
3rd order Arcs
1 Monferrato
2 Emilia
3 Ferrara
4 Adriatic
5 Abruzzi
Fig.1b
a
10°0'0"E
15°0'0"E
45°0'0"N
40°0'0"N
13°0'0"E
14°0'0"E
15°0'0"E
43°0'0"N
42°0'0"N
41°0'0"N
sec.1
sec.2
sec.3
Seismogenic provinces sketch
Moho
Adriatic Arc
Abruzzi Arc
ANCONA
PESCARA
CHIETI
ROMA
ISERNIA
CAMPOBASSO
BENEVENTO
Fig.3
Fig.2
0 25 50 km
b
compression
extension
Lenght as in Fig. 1b
mm/y
dist (km)
topography (m)
c
Strike-slip Province
Contractional Province
Extensional Province
CLASS Seismicity (1981-2018) M_L ≥ 2.0
Sh-min
SH-max
Focal mechanisms
5.0
M_W
6.5

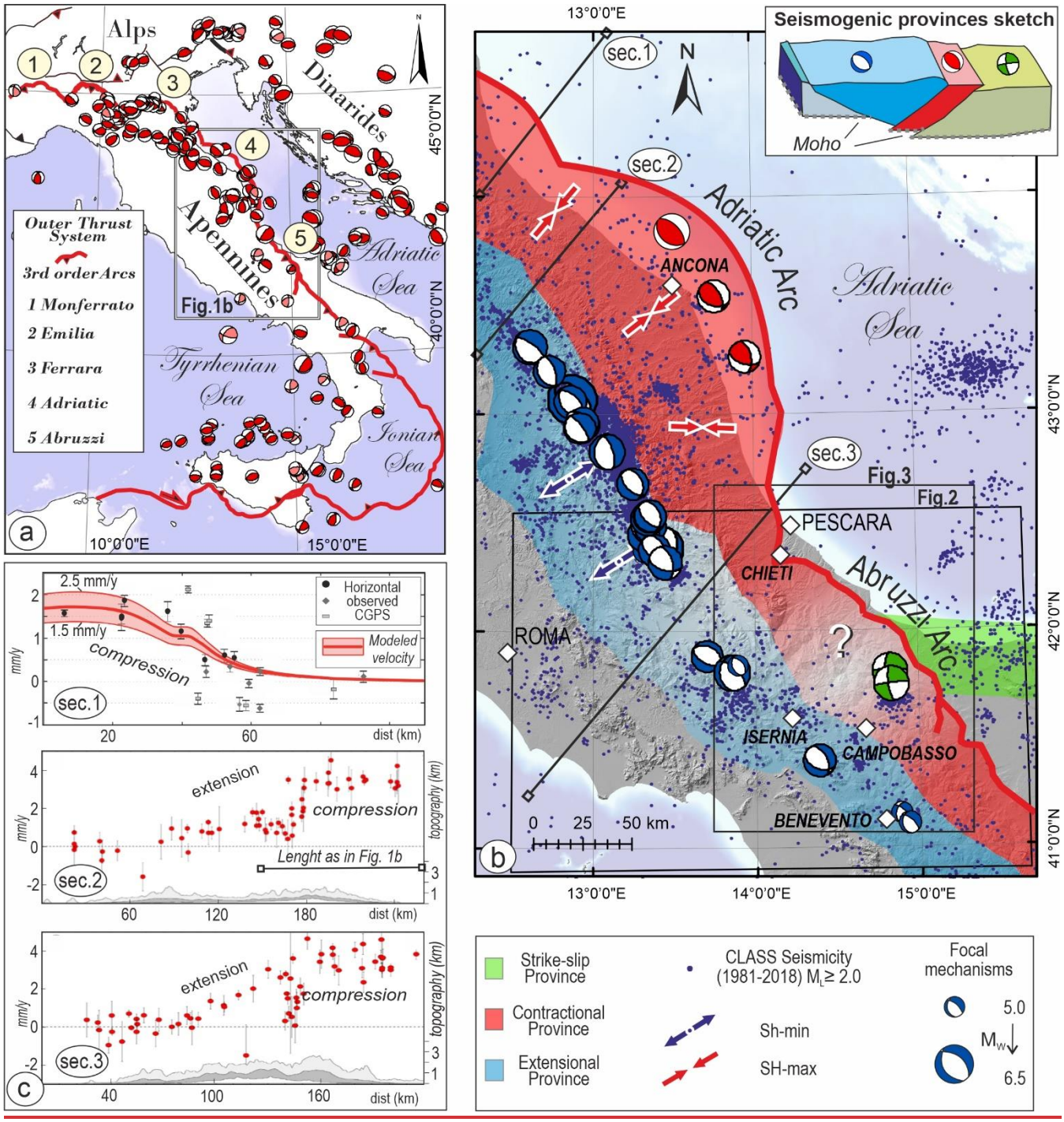

Figure 1. Adriatic and Abruzzi Arc basal thrusts of the Outer Thrust System of Italy (OTS). a) OTS frontal thrust and reverse focal mechanisms from 1960 to 2024 (3.5 ≤ M ≤ 6.1) (Mariucci and Montone, 2022; Scognamiglio et al., 2006). Red focal mechanisms indicate pure reverse faulting, while pink focal ones represent reverse-oblique kinematics b) Quaternary and potentially seismogenic extensional, contractional, and strike-slip provinces in southern-central Italy (modified from Lavecchia et al., 2021b) and

instrumental earthquakes with $M_L \geq 2.0$ (CLASS, Latorre et al., 2023). The beach balls represent the kinematics of earthquakes $M_W \geq 5.0$ (Mariucci and Montone, 2022; Scognamiglio et al., 2006). Key: red = reverse/reverse-oblique fault, blue=normal/normal-oblique fault; green = strike-slip fault. Black lines (sec. 1-3) represent the traces of velocity profiles shown in panel c. The red and blue arrows are the SH-max computed by de Nardis et al. (2022), and the Sh-min provided by Ferrarini et al. (2015). The top right corner inset represents a schematic 3D model of the area's relationship between different tectonic domains. c) GPS horizontal velocity from Pezzo et al. (2020) (~~n.~~sec. 1) and Devoti et al. (2017) (~~n.~~sec. 2, sec. 3).

2 Seismotectonic framework

The Outer Thrust System (OTS) of Italy, which developed during the Late Pliocene to Quaternary at the front of the Apennine–Maghrebian fold-and-thrust belt, represents a first-order arcuate fold-and-thrust system that extends for approximately 2500 km (Figs. 1a, S1). Along its length, the OTS features two second-order, outward-convex arcs: the NNE–ENE–verging Padan–Adriatic arc in the north, and the SE–SSE–S–verging Ionian–Sicilian arc in the south (Lavecchia et al., 2021b). These two arcs are connected by a relatively linear segment in the Southern Apennines. The northern Arc may be subdivided into five third-order arcs, each spanning a few hundred kilometres along strike: Monferrato, Emilia, Ferrara, Adriatic, and Abruzzi (Figs. 1a, S1) (Caputo and Tarabusi, 2016). Regarding the Abruzzi Arc basal thrust, the interpretations vary in the literature. Some authors view it as part of the linear segment connecting the Padan-Adriatic and Ionian-Sicilian arcs (Butler et al., 2004); others consider it as the southern prolongation of the Padan-Adriatic Arc (e.g., Ferrarini et al., 2021a; de Nardis, 2011; Racano et al., 2020). Seismogenic compression along the southern N-S to N10° striking portion of the Adriatic arc and the outer compressional belt of Southern Italy is questioned due to the lack of related instrumental seismic activity; in particular, some authors assume the Abruzzi Arc basal thrust as an inactive compressive structure (Lanari et al., 2023). Geological, seismological, and geodetic evidence support the ongoing thrust activity at least in the Emilia Arc, Ferrara Arc, and the northern portion of the Adriatic Arc (e.g., Govoni et al., 2014; Lavecchia et al., 2023; Tibaldi et al., 2023). Seismic catalogues (e.g., Mariucci and Montone, 2022; Scognamiglio et al., 2006; Italian Seismic Bulletin, ISIDe Working Group, 2007; CLASS, Latorre et al., 2023) indicate that the compressional earthquake activity is mainly concentrated in two depth ranges: a shallower range (0-12 km) and a deeper one (20-25 km).

The Abruzzi Arc basal thrust comprises buried and outcropping east-verging thrust structures that developed during the Late Pliocene–Early Pleistocene, involving the Apulia foreland platform (Di Luzio et al., 2009; Patacca et al., 2008). This compressional domain is bound westward by the Apennine extensional seismotectonic province and eastward by the intra-foreland strike-slip one (Fig. 1b).

Epicentral earthquake maps (Fig. ~~2c~~ 2b, and inset Fig. 3c) reveal an absence of seismicity in the northern Abruzzi sector, with some clustering observed in the central and southern sectors. Based on kinematics and focal depths, these clusters are attributed to the strike-slip province rather than the Abruzzi Arc basal thrust (Fig. 3c, d).

The Apennine extensional province is characterized by NNW-SSE to WNW-ESE striking, normal to normal-oblique faults, Late Pliocene to Quaternary in age (Galadini and Galli, 2000; Lavecchia et al., 2022) (Figs. S3 and S4). The overall system is

125 composed of high-angle westward-dipping segments and moderate to low-angle eastward-dipping segments detaching on a common major eastward deepening basal shear zone (e.g., Brozzetti et al., 2017; Lavecchia et al., 2017). In the past, large earthquakes (Mw ≥ 7.0) (Fig. 2a) struck these portions of the extensional domain, while, in instrumental time, it is characterized by low seismicity rates mostly composed of swarms or minor seismic sequences located mainly at upper crustal depths (< 12–14 km) (Frepoli et al., 2017; de Nardis et al., 2024; Romano et al., 2013b; Trionfera et al., 2019).

130 The strike-slip province consists of E-W structures with right-lateral kinematics and WNW-ESE normal oblique faults dislocating the Adriatic foreland (Argnani et al., 2009; Patacca and Scandone, 2004). These faults outcrop in the Gargano area and are confined to mid-lower crustal depths beneath the Abruzzi Arc basal thrust (e.g., Miccolis et al., 2021) (inset in Fig. 1b, Figs. 2, 3, and S3). Seismic sequences (i.e., San Giuliano 2002, Mw 5.7 and Montecilfone 2018, Mw 5.1, Fig. 3c) struck this area, highlighting the prevailing seismogenic thickness that ranges between 10–20 km (Chiarabba et al., 2005a; Di Luccio et

135 al., 2005). The strike-slip domain is characterized by moderate seismicity rates and significant historical earthquakes (Figs. 1b, 2), contributing to the high seismic hazard of central Italy.

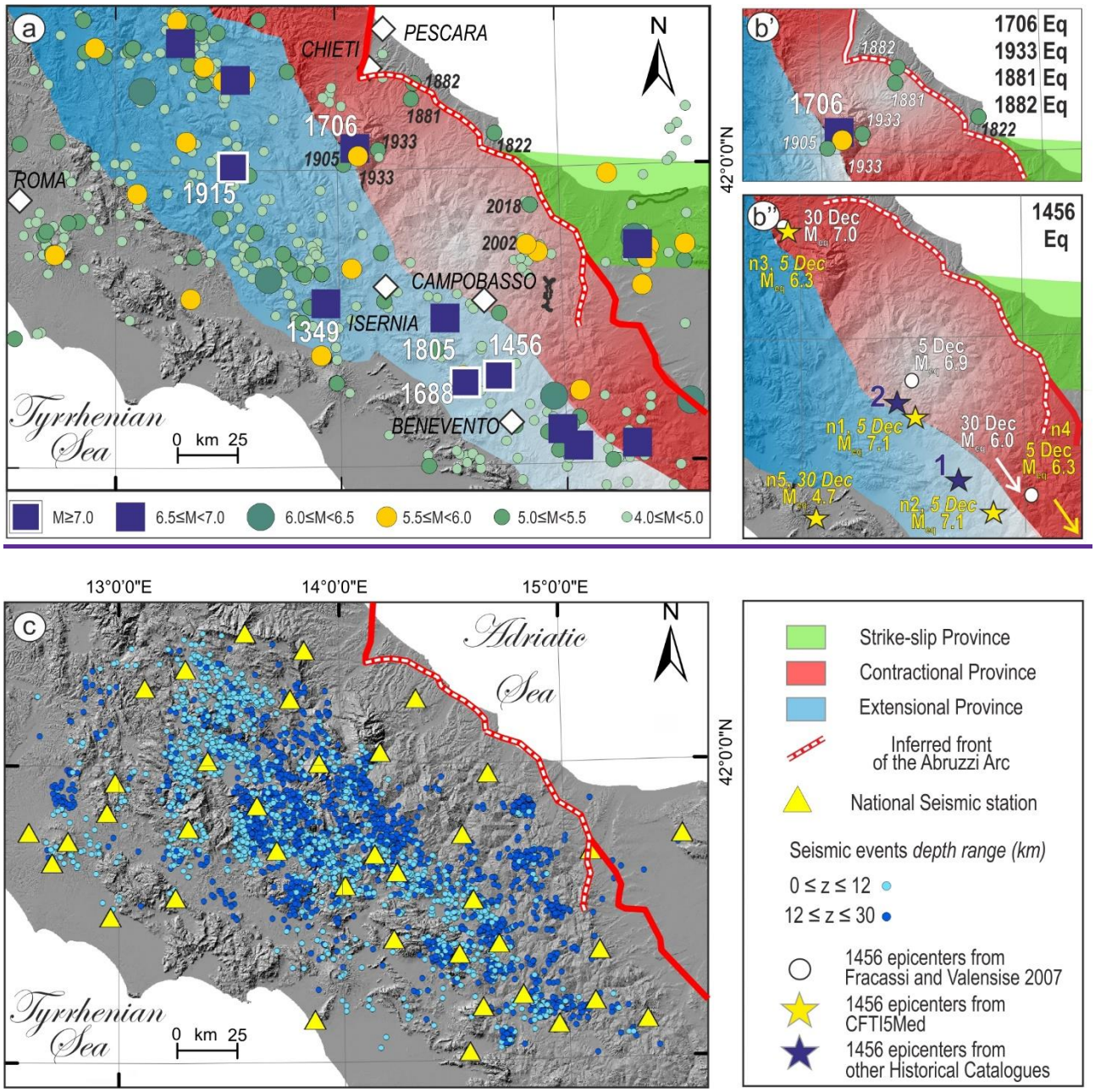
a
CHIETI
PESCARA
ROMA
1706
1915
1905
1933
1882
1881
1822
2018
2002
CAMPOBASSO
ISERNIA
1349
1805
1456
1688
BENEVENTO
Tyrrhenian Sea
0 km 25
N
M≥7.0
6.5≤M<7.0
6.0≤M<6.5
5.5≤M<6.0
5.0≤M<5.5
4.0≤M<5.0
42°0'0"N
b'
1706 Eq
1933 Eq
1881 Eq
1882 Eq
1882
1706
1881
1933
1822
1905
1933
b''
1456 Eq
30 Dec Meq 7.0
n3, 5 Dec Meq 6.3
5 Dec Meq 6.9
2
n1, 5 Dec Meq 7.1
30 Dec Meq 6.0
n4
5 Dec Meq 6.3
1
n5, 30 Dec Meq 4.7
n2, 5 Dec Meq 7.1
13°0'0"E
14°0'0"E
15°0'0"E
c
Adriatic Sea
Tyrrhenian Sea
0 km 25
N
42°0'0"N
Strike-slip Province
Contractional Province
Extensional Province
Inferred front of the Abruzzi Arc
National Seismic station
Seismic events depth range (km)
0 ≤ z ≤ 12
12 ≤ z ≤ 30
1456 epicenters from Fracassi and Valensise 2007
1456 epicenters from CFTI5Med
1456 epicenters from other Historical Catalogues

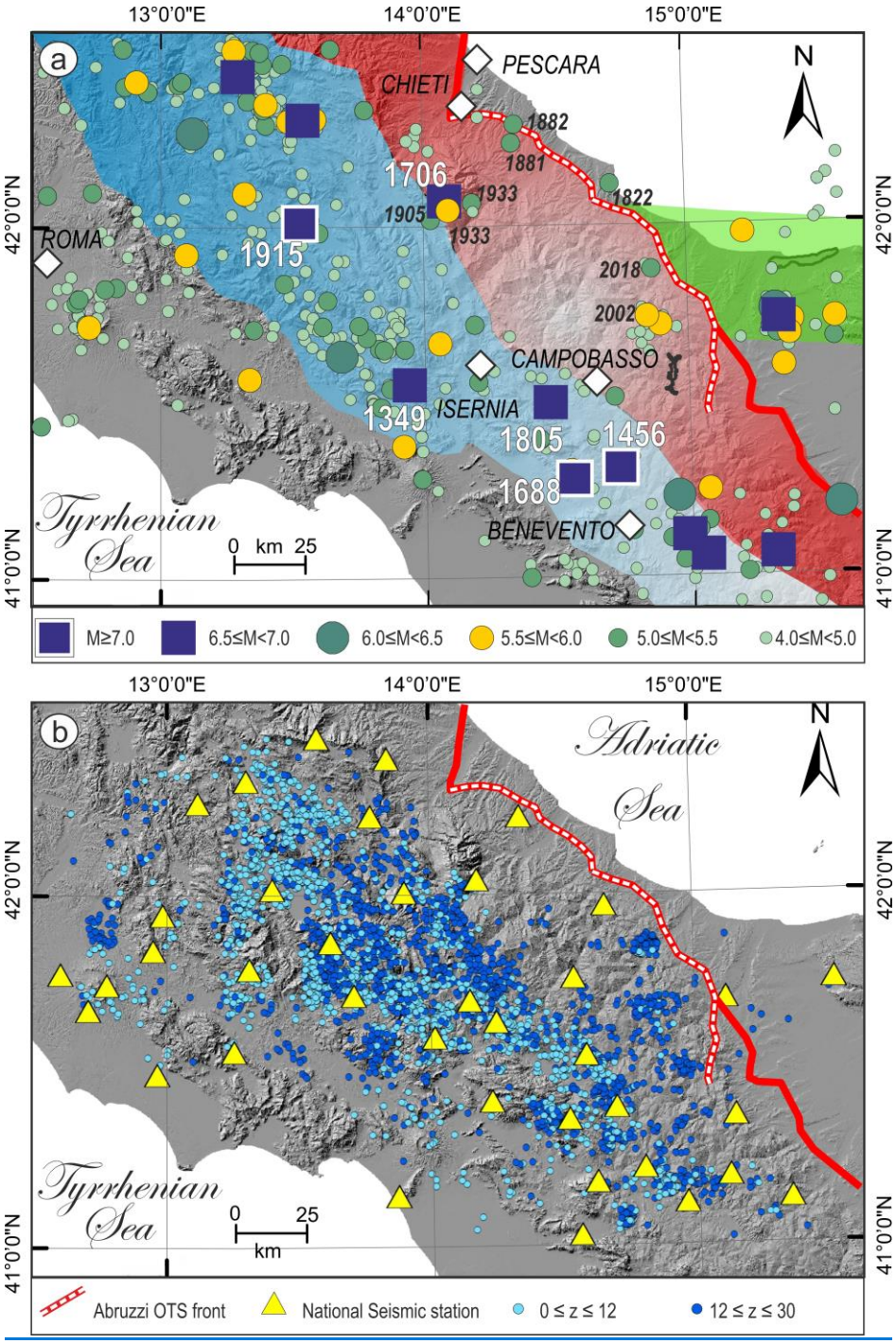

Figure 2. Seismotectonic framework of the tomographic study area. a) Seismotectonic provinces (as in Figure 1b) and major historical ~~earthquakes (CPTI15 v4.0, Rovida et al., 2020, 2022).~~ and instrumental earthquakes from the CPTI15 v4.0 catalogue (Rovida et al., 2020, 2022), spanning the period 1000–2020. ~~b) Focus on historical earthquakes with uncertain fault association (see Fig. S2 for the macroseismic fields of the earthquakes labelled in b'); b') Historical earthquakes in the northern Abruzzi Arc basal~~

~~thrust, b'') Macroseismic epicentres for the 1456 earthquake as proposed in the literature. The blue star represents the solution from CPTI15 v4.0, (Rovida et al., 2020, 2022), which reports it as a single event. The yellow stars and white circles refer to Guidoboni et al. (2018, 2019) and Fracassi and Valensise (2007), respectively, who consider it a multiple event. M stands for equivalent magnitude. eb~~) **Distribution of earthquakes and seismic stations used for the travel time tomography (January 2009 – December 2020, $0.2 \leq M_L \leq 5.5$).**

3 Materials and Methods

3.1 Seismological data

To perform a travel-time seismic tomography, we use events from the ISIDe database (ISIDe Working Group, 2007) located in and around the Abruzzi Arc basal thrust and nearby seismotectonic provinces. The selected earthquakes have a station-event geometry that ensures good ray coverage across the tectonic structures investigated (Fig. ~~2c~~2b).

Our initial dataset consists of P- and S-wave arrival times from approximately 20,600 events ($0.2 \leq M_L \leq 5.5$), recorded by 37 stations of the Italian National Seismic Network between January 2009 and December 2020 (Fig. S5). These earthquakes are located within a rectangular region defined by latitudes 41.00°–42.50°N and longitudes 12.60°–15.60°E, at depths ranging from 0 to 30 km (~~Figure~~ Fig. 2~~b~~e). To refine the dataset, we only selected events with more than 10 P- and S-wave arrival times. This criterion excludes events with poorly constrained hypocentres and therefore reduces mislocation errors in the tomographic process (Fig. S6).

We then performed a preliminary relocation of these events using three different 1D velocity models proposed for the study area (Frepoli et al., 2017; Romano et al., 2013b; Trionfera et al., 2019) (Figs. S7-S8). We evaluated the quality of each resulting catalogue based on the criteria of Michele et al. (2019) and selected the one with the best-constrained locations (~~using the model of~~ Trionfera et al. ~~(~~2019). Lastly, we applied a final quality filter, removing all events with a root mean square (RMS) of travel-time residuals greater than 0.5 s or an azimuthal gap greater than 180°. The final dataset comprises 42,176 P- and 29,045 S-wave arrival times from 5,712 earthquakes.

In addition, we revise microseismicity calculating new focal mechanisms ~~use seismicity distribution and available focal mechanisms~~ to interpret and contextualize the resulting 3D Vp, Vs models. For this purpose, we take into consideration ~~1)~~ an unpublished seismic catalogue from a temporary seismic network experiment (Romano et al., 2013a, b) ~~and 2) the Italian earthquake catalogue CLASS (Latorre et al., 2023) (Fig. 3).~~ . This catalogue, together with the catalogue from Chiarabba et al. (2005), have been referenced for local seismotectonic details, while the CLASS database (Latorre et al., 2023) spanning from 1981 to 2018 is used as reference of the seismic activity of the area.

3.2 Travel time tomography

We perform the seismic travel time tomography with the Fast-Marching Tomography algorithm FMTOMO (Rawlinson and Sambridge, 2006; Rawlinson and Urvoy, 2006). FMTOMO performs forward modelling using the fast-marching method ~~(FMM)~~ to solve the eikonal equation on a regular grid (propagation grid), providing stable and efficient estimates of first-arrival travel times in heterogeneous media. Ray paths are then reconstructed by back-tracing along the normal to the wavefront in each step~~, steepest gradient of the travel time field, allowing~~. ~~t~~The computation of Fréchet derivatives ~~that~~ relates travel-time residuals to velocity perturbations. The inversion is carried out on a separate grid (velocity grid), which defines the parame~~t~~rization of the model. The use of a finer propagation grid allows accurate computation of travel times and ray paths, while the coarser velocity grid reduces the number of free parameters. FMTOMO follows an iterative and linearized approach: at each step, travel-time residuals are minimized to obtain a velocity model update through a ~~regularized least squares optimization~~subspace inversion, incorporating damping and~~/or~~ smoothing constraints. The process is iterated, with each updated model used as the input for a new round of fast-marching travel-time calculation and ray reconstruction, until the data misfit stabilizes. To ensure good coverage of seismic rays along the contractional domain, we enlarge the study area as shown in the Figure~~.~~ 2~~b~~e, including the innermost extensional and the easternmost strike-slip domains. As a starting model for the travel time tomography, we use the 1D velocity profile proposed by Trionfera et al. (2019) in the Figure~~.~~ S~~8~~7. The propagation grid spacing is about 2 km along the depth and 5 km in latitude and longitude. ~~The propagation grid~~It extends 4.5 km above sea level to a depth of 31.5 km, with boundary surfaces at 4 km and 31 km, respectively. Sources and receivers are required to be inside the layer bounded by these two surfaces: maximum height of stations (above the sea) is about 1.8 km, while earthquakes are filtered with depth ≤ 30 km (below the sea). The chosen values allow to include all earthquakes and stations by ensuring also a buffer zone of 1 km to avoid boundary effects. ~~The grid spacing is about 2 km along the depth and 5 km in latitude and longitude.~~ We estimate the inversion parameters through classical trade-off curves (Fig. S~~8~~9), obtaining the best damping value of 25 and the best smoothing value of 5. We invert only the 3D seismic velocity, using ~~an inversion~~ a velocity grid spanning the same depth range, about 3 km of vertical and 8 km of horizontal spacing. The resolution and reliability of the obtained tomographic models have been verified through a synthetic checkerboard and targeted spike tests (Figs. 4, S10~~9~~, ~~-~~ ~~S10~~S12). ~~Further details are given in Appendix A~~.

3.3 Focal Mechanism Solutions

We compute seven new focal mechanisms (Figs. 3~~b~~c, ~~S11~~S13) by selecting the most significant seismic events (M_L 2.4-3.8) possibly associated with the Abruzzi Arc basal thrust utilizing the seismic phases of a temporary seismic network installed from 2009 to 2011 for local monitoring purposes (Romano et al., 2013a). We integrate the waveforms recorded by the local temporary seismic network (Romano et al., 2013a, b) with those recorded by the National Seismic Network, and we invert P polarities by using the FPFIT code (Reasenberg and Oppenheimer, 1985).

We considered only the seismic events with more than 9 polarity readings. From this dataset, we selected the best solutions based on 1) the uniqueness of the solution and 2) two quality factors (Q) provided by the code: the degree of polarity misfit (Qf) and the uncertainty range of strike, dip, and rake (Qp). Solution quality decreases from A to C.

~~We select the best solutions from this data set based on two quality factors (Q) provided by the code itself, i.e., the degree of polarity misfit (Qf) and the range of the strike, dip, and rake uncertainties (Qp) for each solution; from A to C, the quality decreases.~~ We also collect FMS for the study area from Milano et al. ~~(2005), Montone and Mariucci (2023), Pondrelli et al. (2006), and Scognamiglio et al. (2006).~~

3.4 Geological and geophysical material

We collect available geological and structural maps and multi-scale cross-sections based on interpreted seismic lines and/or balancing techniques. Specifically, we compile a georeferenced database for the study area that includes: the Structural Model of Italy (scale 1:500.000) (Bigi et al., 1992), Geological Sheets from Carta Geologica d'Italia at scales of 1:100.000 and 1:50.000, deep wells from the VIDEPI database (www.videpi.com), maps and sections from Adinolfi et al. (2015), Brozzetti (2011), D'Ambrosio et al. (2021), Ferrarini et al. (2017), Ghisetti et al. (1993), Ghisetti and Vezzani (2002), Lavecchia et al. (2021b), Mostardini and Merlini (1986), Patacca et al. (2008), Romano et al. (2013b), and Vezzani et al. (2010). We also integrated the tomographic and geophysical maps from Bisio et al. (2004), Chiarabba et al. (2010, 2020), Di Stefano et al. (2011), Improta et al. (2014), Scafidi et al. (2009), and Speranza and Chiappini (2002).

The compilation also includes strike-slip faults in the Adriatic foreland, east-dipping master faults along the western boundary of the Apennine extensional province, and the outermost outcropping west-dipping normal faults at the eastern boundary of the extensional province (Figs. 3a, S3). The fault traces were derived from QUIN 1.0 and QUIN 2.0 host fault databases (Lavecchia et al., 2021a, 2023a), Battistelli et al. (2025), Ferrarini et al. (2021b), and Talone et al. (2023).

A comprehensive summary of the geological and geophysical datasets is provided in the Supplementary Material (Fig. ~~S12~~S14).

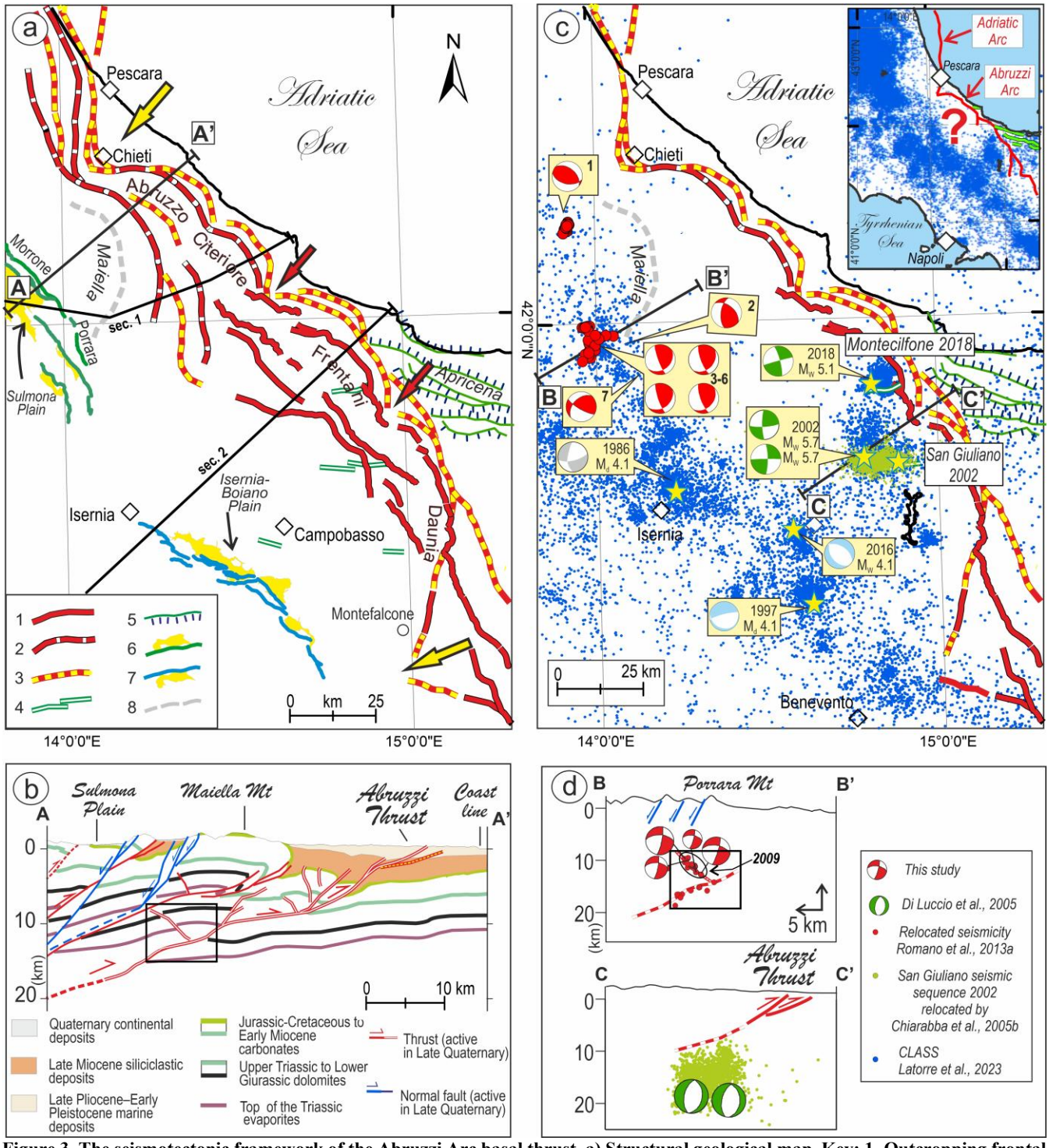

Figure 3. The seismotectonic framework of the Abruzzi Arc basal thrust. a) Structural geological map. Key: 1. Outcropping frontal and oblique thrusts of Quaternary age within the Apennine foothills and coastal area. 2. Blind outermost splays of the Abruzzi thrust system. 3. Buried thrust structures with hints of activity from topographic relief and fluvial network analysis (after Ferrarini et al.,

2021a). 4. Right-lateral strike-slip structures from earthquake data at middle crust depth. 5. Outcropping Quaternary oblique strike-slip faulting in the Adriatic foreland. 6. Morrone-Porrara west-dipping normal fault system. 7. Bojano east-dipping normal fault system. 8. Maiella thrust front. The yellow arrows point to the northern and southern terminations of the Abruzzi Arc basal thrust; the small red arrows highlight its segmentation into three fourth-order arcs (Abruzzo Citeriore, Frentani, Daunia) as reconstructed in this paper. The black lines named sec.1 and sec.2 represent the traces of the geological sections from CROP11 (Patacca et al., 2008)) and Butler et al. (2004), respectively. b) Regional cross-section after Ferrarini et al. (2021a). The trace A-A' is shown in panel a~~, and b~~. ~~Red circles and green-blue contour lines as in legend panel d.~~ c) The seismicity distribution, from 1981 to 2018 (CLASS, Latorre et al., 2023), is represented by blue dots. Red and green circles indicate relocated seismic events from Romano et al. (2013a) and (~~Chiarabba et al.~~, (2005b), respectively~~; Romano et al., 2013a~~). The focal mechanisms of the most significant events are from Milano et al. (2005), Montone and Mariucci (2023), Pondrelli et al. (2006), and Scognamiglio et al. (2006). The focal mechanisms, labelled 1–7, are from this study. (d) Cross-sections B-B' and C-C' represent the depth distribution of the relocated events by Romano et al. (2013a) and Chiarabba et al. (2005b) and the respective focal mechanism in section view. ~~of seismicity represented by dots and kernel density. The histogram and probability density functions (PDF) illustrate the hypocentral depth distribution along the C-C' cross-section (green and blue dots).~~

3.5 Model building

For building a comprehensive conceptual 3D fault model, we integrated seismic tomography results with ~~seismicity distribution and~~ geological-geophysical data following the approach from the Community Fault Model of Southern California (Nicholson et al., 2014; Plesch et al., 2007), adapted for a buried thrust context (de Nardis et al., 2024; Tibaldi et al., 2023). The procedure includes four main steps:

1) Geological Mapping: We delineated the traces of outcropping and buried thrust structures of the southern Adriatic Arc and Abruzzi Arc basal thrust using multi-source geological data compiled within a GIS platform (Fig~~s~~. 3).

2) Shallow 3D Extrusion: Using MOVE suite (Petroleum Experts Ltd., version 2022.1), we extruded the fault traces of the Abruzzi Arc basal thrust up to 5 km. The same approach was adopted for strike-slip faults and normal faults, extending them along their dip to the base of the seismogenic layer (Latorre et al., 2023). Average dip angles were derived from geological cross-sections and regional transects as well as from data in the QUIN 1 and QUIN 2 fault/striation pair databases (Lavecchia et al., 2021a, 2023a).

3) Cross-Section Construction: We constructed a grid of serial vertical cross-sections spaced ~~18~~ 9 km apart and oriented N10°E, N40°E, and N60°E across the tomographic model (~~Fig. 5~~6, Figs S17-S28). The geometry of the Abruzzi Arc basal thrust was traced wherever identifiable in the velocity models ~~(see Supplementary material for details,)~~. Then we connect ~~by connecting~~ the shallow depth extruded fault surfaces with deeper thrust features inferred from tomographic evidence of crustal doubling (purple lines in Fig. 7a). Each section was further refined using published geological transects in ~~(~~ Fig~~.~~ure ~~S12~~S14~~.)~~.

4) 3D Interpolation: We generated a non-planar surface of the Abruzzi Arc basal thrust down to ~24 km by interpolating its traceable segments across multiple cross-sections using the Delaunay triangulation method (Delaunay, 1934; Okabe et al., 1992). Smoothed depth contour lines were extracted at 2 km intervals (dotted red lines in Fig. 7~~6~~c).

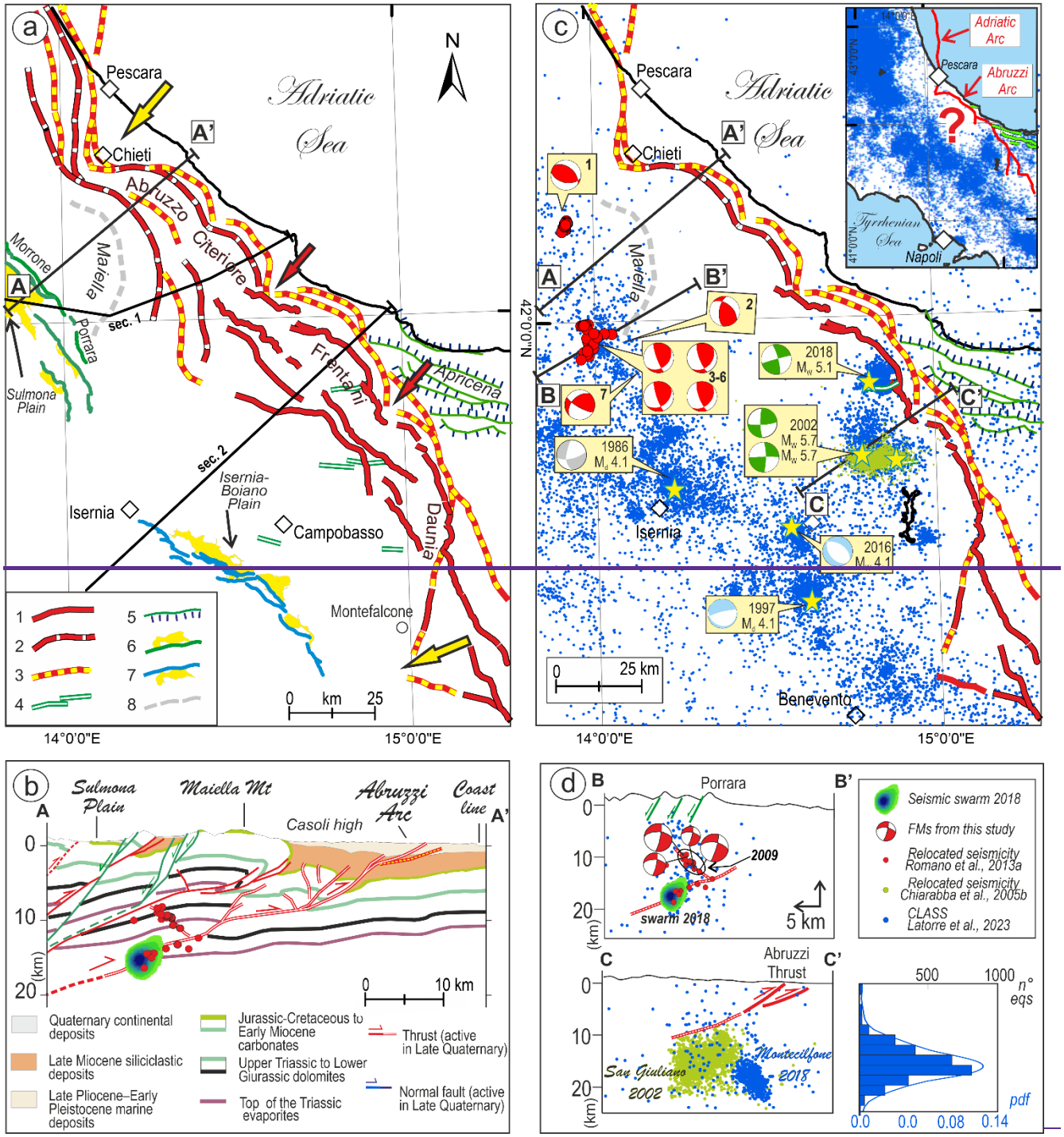

~~**Figure 3. The seismotectonic framework of the Abruzzi Arc basal thrust. a) Structural geological map. Key: 1. Outcropping frontal and oblique thrusts of Quaternary age within the Apennine foothills and coastal area. 2. Blind outermost splays of the Abruzzi thrust system. 3. Buried thrust structures with hints of activity from topographic relief and fluvial network analysis (after Ferrarini et al., 2021a). 4. Right-lateral strike-slip structures from earthquake data at middle crust depth. 5. Outcropping Quaternary oblique strike-slip faulting in the Adriatic foreland. 6. Morrone-Porrara west-dipping normal fault system. 7. Bojano east-dipping normal fault**~~

~~system. 8. Maiella thrust front. The yellow arrows point to the northern and southern terminations of the Abruzzi Arc basal thrust; the small red arrows highlight its segmentation into three fourth-order arcs (Abruzzo Citeriore, Frentani, Daunia) as reconstructed in this paper. The black lines named sec.1 and sec.2 represent the traces of the geological sections from CROP11 (Patacca et al., 2008)) and Butler et al. (2004), respectively. Red circles and green-blue contour lines as in legend panel d. b) Regional cross-section after Ferrarini et al. (2021a). The trace A-A' is shown in panel a, and b. c Red circles and green-blue contour lines as in legend panel d. c) The seismicity distribution, from 1981 to 2018 (CLASS, Latorre et al., 2023), is represented by blue dots. Red and green circles indicate relocated seismic events (Chiarabba et al., 2005b; Romano et al., 2013a). The focal mechanisms of the most significant events are from Milano et al. (2005), Montone and Mariucci (2023), Pondrelli et al. (2006), and Scognamiglio et al. (2006). The focal mechanisms, labelled 1–7, are from this study. (d) Cross-sections of seismicity represented by dots and kernel density. The histogram and probability density functions (PDF) illustrate the hypocentral depth distribution along the C–C' cross-section (green and blue dots).~~

~~5~~4 Parametrization and Model Resolution

We optimized the grid parametrization as node spacing directly controls the maximum resolvable wavelength of the model (i.e., the smallest constructible anomaly size).

Starting from a reference grid (2.5 x 2.5 x 2.5 km), we propagated the wavefront using progressively coarser and finer grid configurations. For each configuration, we evaluated the relationship between cell volume and data root mean square (RMS) misfit (Fig. S9). We defined the optimal grid spacing as half the average distance to the nearest seismic station in the horizontal direction and half the standard deviation (σ) of the earthquake depth distribution in the vertical direction. This resulted in a horizontal spacing of 5 km and a vertical spacing of 42 km, which minimizes the residual RMS. We determined the number of iterations adopted for both P- and S-wave velocity models (12 iterations) based on the stabilization of the residual reduction. After that, we computed classical trade-off curves to estimate the optimal regularization parameters (damping and smoothing) by balancing data misfit and model roughness (Fig. S~~8~~9). For each parameter combination, the tomographic inversion was iterated three times. The optimal values were selected at the point of maximum curvature on the trade-off curves, yielding a damping value of 25 and a smoothing value of 5.

Given the non-uniqueness of the tomographic inversion, we assessed model resolution and reliability using synthetic checkerboard and spike tests. We calculated synthetic travel times using the same source–receiver geometry as the observed data and added a random noise with a priori covariance to the data to simulate the arrival time uncertainties.

We designed checkerboard tests to evaluate sensitivity to anomalies of different sizes. We tested three checkerboard dimensions, corresponding to 10 × 10 × 8 km (finer size), 15 × 15 × 12 km (medium size), ~~,~~ and 20 × 20 × 16 km (coarser size), respectively (Fig. 4 and Figs S10 – S11).

The results indicate that S-wave models resolve sharper velocity contrasts than P-wave models, which exhibit smoother anomaly patterns. The best recovery appears at the medium and coarser checkerboard, particularly at shallower to medium depths (Fig. 4 and Figs S10-S11).

The non-uniform depth distribution of earthquakes results in heterogeneous ray coverage at intermediate depths. Consequently, the number and angular distribution of rays crossing each cell allow a reliable reconstruction of coarser anomalies, whereas resolution is reduced for intermediate checkerboard sizes at depths of approximately 10 km. We also recover larger-scale anomalies below 20 km depth, while finer-scale structures lose resolution. The smallest anomalies are resolved only at shallow depths beneath the chain area.

Overall, the checkerboard tests indicate that the minimum resolvable anomaly size in the final models is approximately 15 km, with locally smaller values (see Fig. 4 and Figs S10 – S11). Accordingly, we focus the interpretation on smaller-scale anomalies only at shallow depths, where we estimate a resolution on the order of 10 km. Other velocity features discussed in this study are comparable in size to the medium and coarse checkerboard anomalies that are well resolved in the study area. We do not interpret additional anomalies present in the models where their size or location falls outside the resolvable domain defined by the synthetic tests.

Targeted spike tests were performed after the tomographic process to check the reliability and resolution of the deeper features presented and analysed in this study. We introduced synthetic velocity perturbations of ±2 km s^{-1} into the initial 1-D reference model, reproducing the geometry of the main observed features (Figs. S12). We tested both original- and reverse-polarity configurations to verify the capability of the inversion to image velocity variations and to exclude artifacts related to ray geometry (Rawlinson and Spakman, 2016).

Despite the decrease in checkerboard resolution with depth, the spike tests indicate that we resolve the model down to approximately 24 km depth, especially for the larger-scale anomaly. Considering the spike tests, the main features are recovered up to 24 km, loosing resolution below this depth.

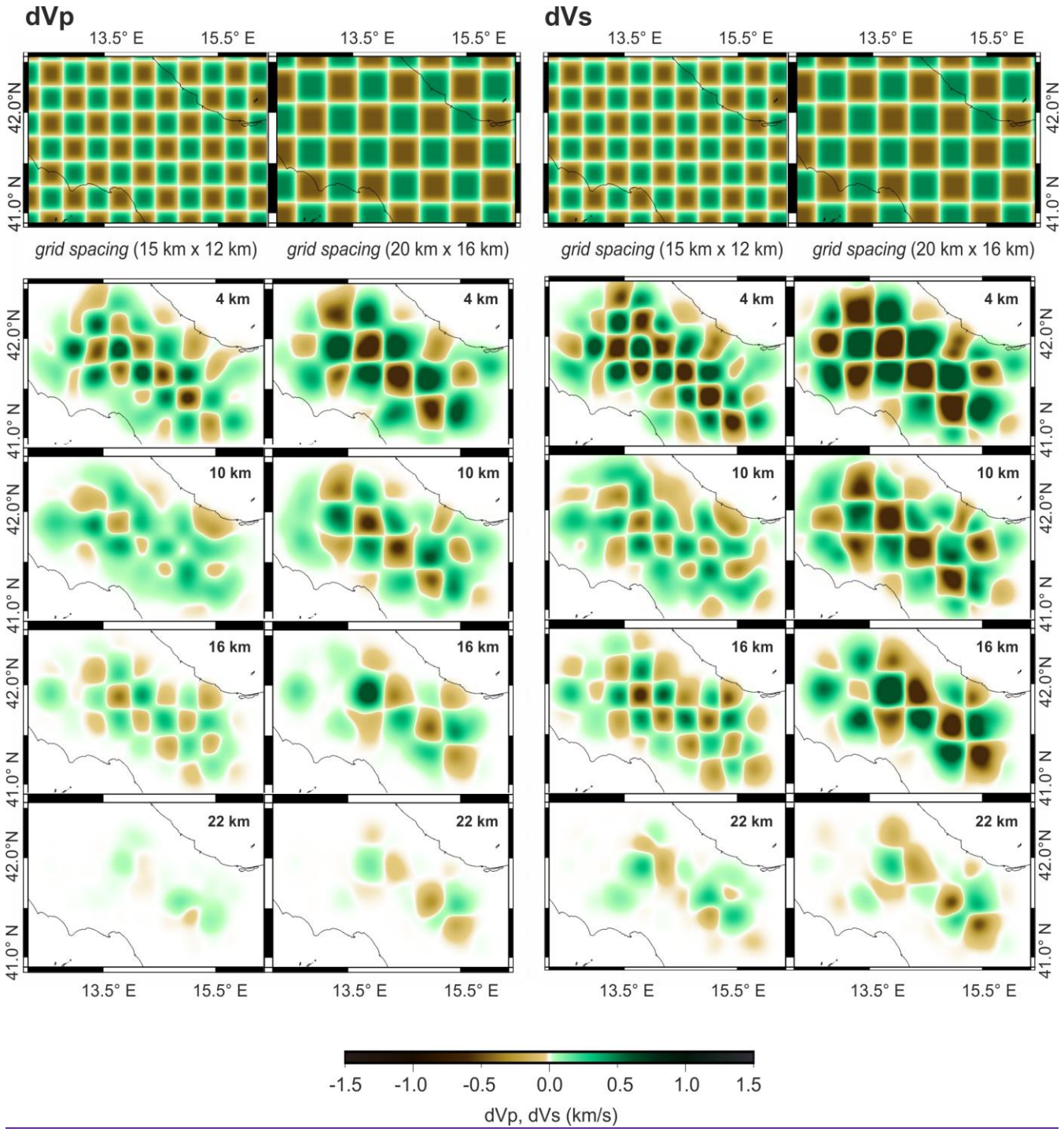
dVp
dVs
13.5° E
15.5° E
42.0°N
41.0° N
grid spacing (15 km x 12 km)
grid spacing (20 km x 16 km)
4 km
10 km
16 km
22 km
-1.5
-1.0
-0.5
0.0
0.5
1.0
1.5
dVp, dVs (km/s)

Figure 4. P- (left) and S (right) model checkerboard tests….. are represented on a horizontal section by cutting the model each 6 km (depth is reported top-right into the map). The two columns show a different size of the checkerboard cells: in the first one, the medium checkerboard is 15 km horizontal and 12 km vertical; in the second one, the coarser cells are 20 km horizontal and 16 km vertical. Seismic velocity is represented as a variation in km/s from uniform fixed values of 3.4 km/s (median of the 1D starting velocity model)

5 Results

45.1 Local Earthquake Tomography

The local earthquake tomography enables the definition of Vp and Vs velocity models in central-southern Italy. Both our models (well resolved down to 20 and locally up to ~24 km) provide great confidence, with a reduction of RMS and covariance of ~73% and ~93% for Vp, and ~65% and ~88% for Vs (Fig. ~~S8~~S9). The final RMS values obtained are about 0.2-0.3s for both the P and the S models (Fig. S9), which is quite better compared to the original RMS distribution of the relocated catalog filtered to be <= 0.5 s (see Fig. S6 for details) The different velocities agree with the anomalies' overall attitude, exhibiting low fluctuation in the Vs relative to the Vp. For building the 3D fault model, both the results of P- and S-waves are considered, but for the sake of simplicity, only the Vp results are shown in cross sections (Figs. 5-6), as they are also meaningful for the lithological aspects. To validate the reliability of these velocity values, we compare them with those in the available literature, for which a correlation with lithology has been provided (Bisio et al., 2004; Chiarabba et al., 2010, 2020; Di Luzio et al., 2009; Improta et al., 2014; Trionfera et al., 2019; Trippetta et al., 2021). The seismic velocity pattern is examined on horizontal slices at different depths (see Figs. 54, S1~~3~~5 and S146) and cross sections with variable direction and spacing (Figs. 6~~5~~, S17 – S28). The Vp and Vs velocity models reveal scattered but circumscribed low-velocity anomalies (Vp < 5 km/s, Vs < 3 km/s) in the upper crust (from the surface to a maximum depth of 8 km), both within the intra-Apennine extensional domain (n. 1, 2 in Fig. 45), and at the hanging wall of the buried Abruzzi Arc basal thrust (n. 3, 4, 5, 6, 7 in Fig. 54). The low-velocity anomalies in the Apennine extensional domain are discontinuous. They are mainly aligned within the western east-dipping and the eastern west-dipping envelopes of normal extensional faults (i.e., the extensional domain boundaries, represented in Figs. 1b, 2a, and S3). Although the inversion grid gives them a bubble shape (due to the interpolation method and the grid spacing), the geographical position and the values of both Vp and Vs velocities correlate well with the presence of Quaternary intra-mountain basins typical of these areas (e.g., Fucino and Sulmona basins in Figs. S3).

Moving eastward, we observe low-velocity zones east of the extensional domain, at the hanging wall of the Abruzzi Basal Thrust. Specifically, we recognize five anomalies (n. 3, 4, 5, 6, 7 in Fig. 54) likely related to lithological variation between 2 and 8 km. Anomalies 3 and 4 can be correlated with coastal facies and fluvial deposits typical of the peri-Adriatic zone, and anomalies 5, 6, and 7 are associated with both sandstone and clay units, Miocene to Pleistocene in age (see the lithological map in Fig. S4).

Anomalies 5 and 6 do not correlate with clear tectonic structures and persist at depths of approximately 8–10 km. Their location corresponds to a large positive magnetic anomaly (Speranza and Chiappini, 2002), the origin of which is still debated. The authors speculate that magmatic rocks may be present either within the basement or trapped in the sedimentary sequences.

While our findings cannot resolve the lithological nature of these rocks, the tomographic anomaly is constrained within the upper 10 km. Therefore, assuming that magmatic rocks exhibit higher seismic velocities than sedimentary ones, we favour the hypothesis of a deeper magnetic source as the cause of the positive magnetic anomaly.

The most significant feature revealed by local seismic tomography is a broad velocity inversion imaged at depths between ~14 and 24 km, within the area bounded by latitudes 41.3°–41.8° and longitudes 14.3°–15.0° (n. 8 and 9 in Fig. 54). Given its considerable lateral extent (see Fig. 56) and the possible loss of resolution at these depths, the reliability of these features is properly tested and confirmed through synthetic analysis (i.e., the spike test represented in Fig. S10S12). This result delineates a well-developed doubling zone, featuring a lower-velocity layer (6.0–6.6 km/s) beneath a higher-velocity layer (6.6–7.0 km/s), a configuration consistent with a mid-crustal overthrust system where a stack of crystalline and Mesozoic units overrides a lower-velocity footwall likely composed of Triassic evaporites and Verrucano formations.

A comparable high-velocity body was documented slightly north of our study area by Chiarabba et al. (2010), who interpreted it as the result of mid-crustal thrust imbrication involving dolomitic lithologies. While their model emphasizes the high-velocity domain, it lacks the depth resolution necessary to resolve the underlying low-velocity structure imaged in our study. We consider the two models fully compatible and integrable into a coherent framework, provided that the high-velocity body is interpreted as the hanging-wall block, and the low-velocity inversion highlighted in our tomographic model is recognized as the footwall.

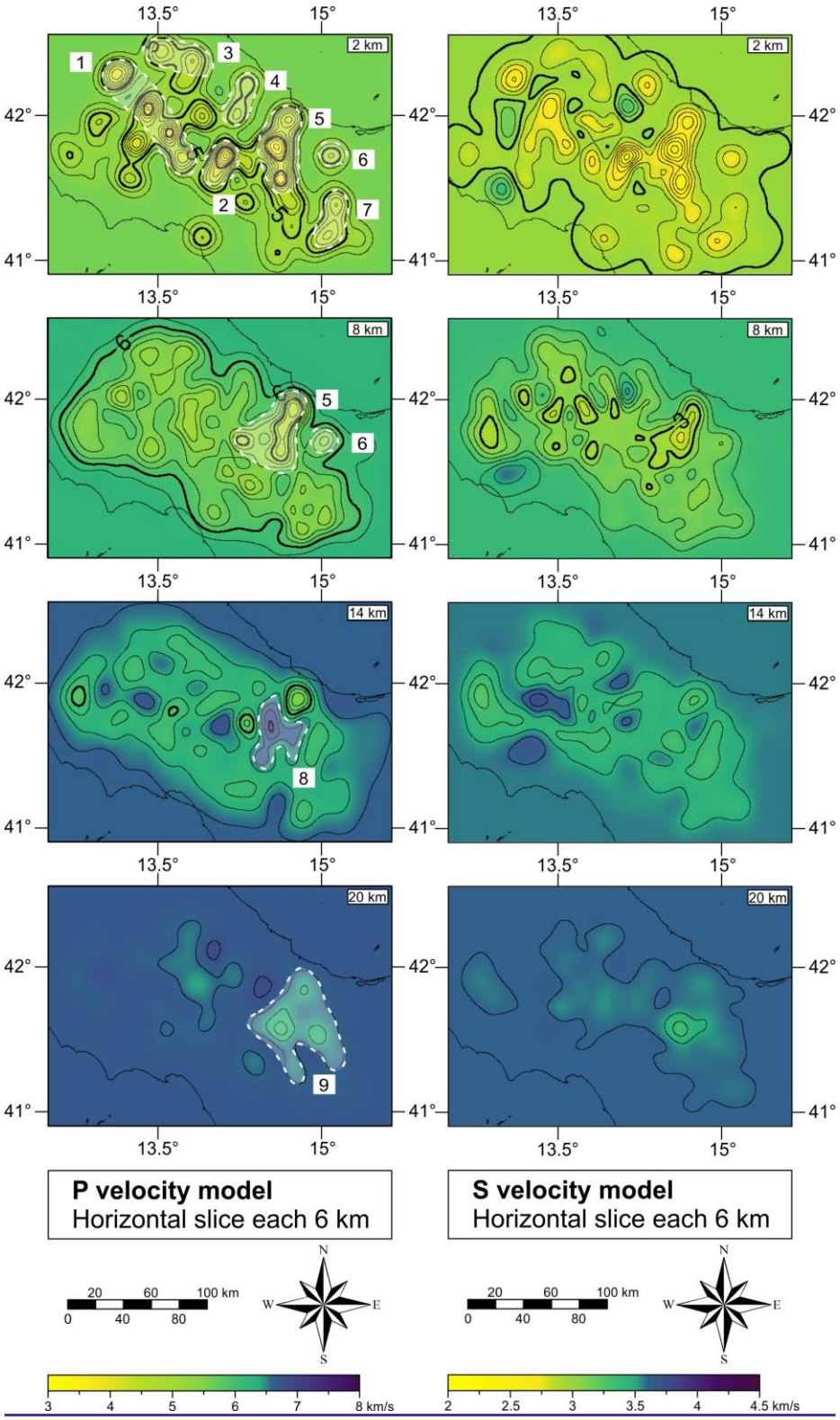
13.5°
15°
42°
41°
2 km
8 km
14 km
20 km
1
2
3
4
5
6
7
8
9
P velocity model
Horizontal slice each 6 km
S velocity model
Horizontal slice each 6 km
20 60 100 km
0 40 80
N
W
E
S
3 4 5 6 7 8 km/s
2 2.5 3 3.5 4 4.5 km/s

380

Figure 4. Horizontal slices crossing the tomographic models at each 6 km. The first column represents the P-wave velocity~~,~~ and the second refers to the S-wave velocity~~, and the third depicts the Vp checkerboard~~. The numbers from 1 to 9 point at the velocity anomalies discussed in the text.

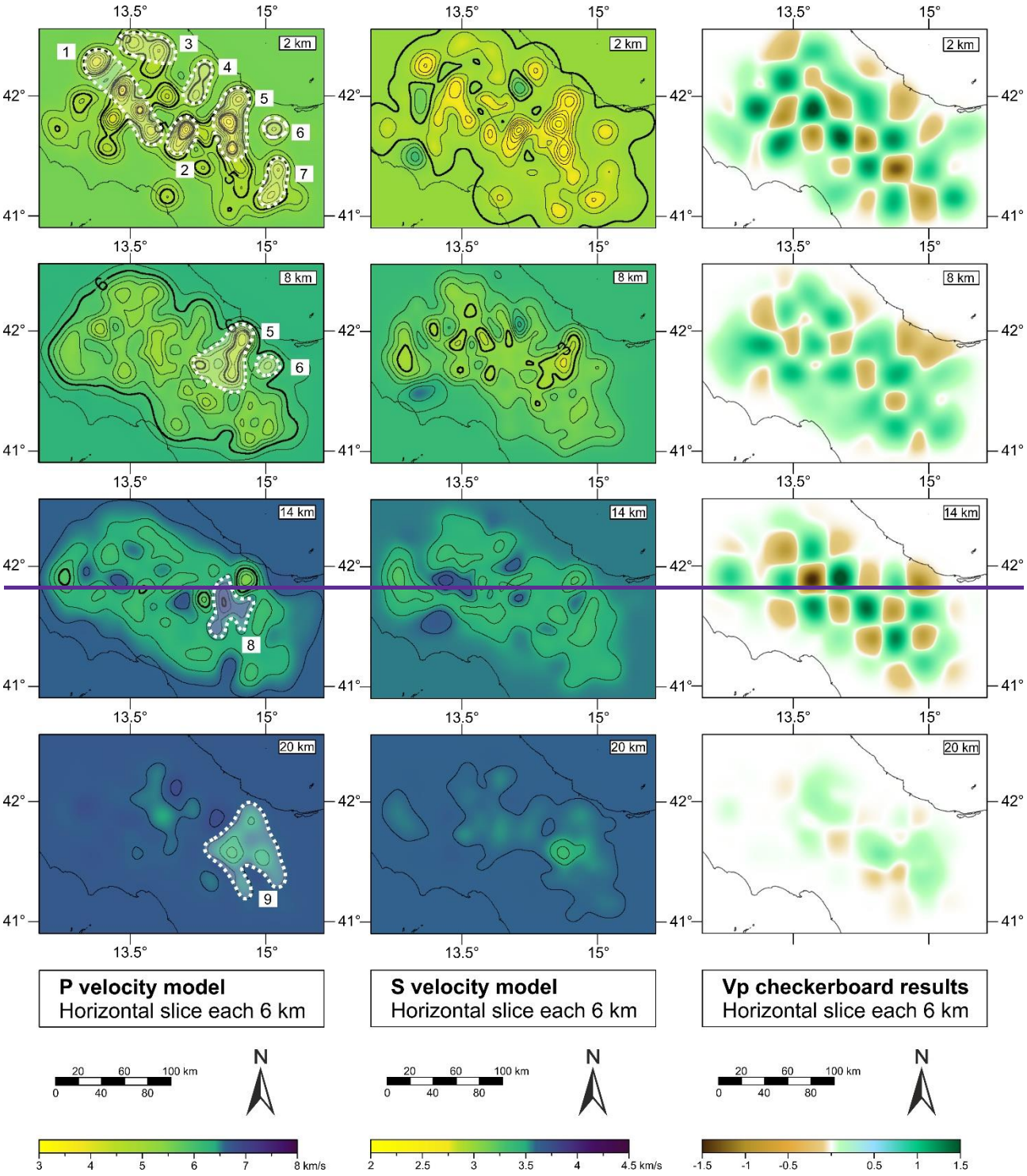
13.5°
15°
42°
41°
2 km
8 km
14 km
20 km
1
2
3
4
5
6
7
8
9
P velocity model
Horizontal slice each 6 km
S velocity model
Horizontal slice each 6 km
Vp checkerboard results
Horizontal slice each 6 km
20 60 100 km
0 40 80
N
3 4 5 6 7 8 km/s
2 2.5 3 3.5 4 4.5 km/s
-1.5 -1 -0.5 0.5 1 1.5

385

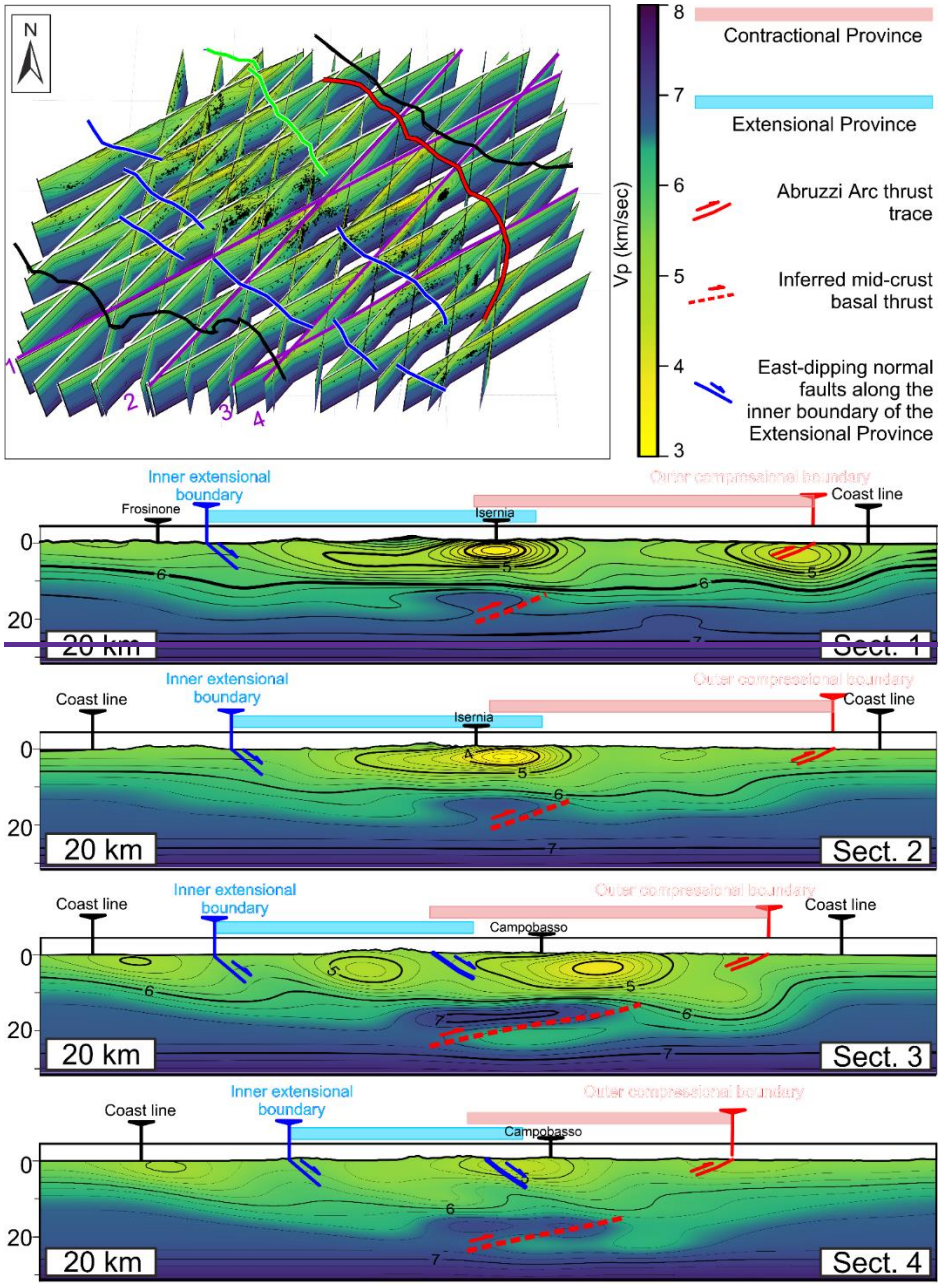
N
1
2
3
4
Vp (km/sec)
8
7
6
5
4
3
Contractional Province
Extensional Province
Abruzzi Arc thrust trace
Inferred mid-crust basal thrust
East-dipping normal faults along the inner boundary of the Extensional Province
Inner extensional boundary
Outer compressional boundary
Frosinone
Isernia
Coast line
Campobasso
0
20
20 km
Sect. 1
Sect. 2
Sect. 3
Sect. 4

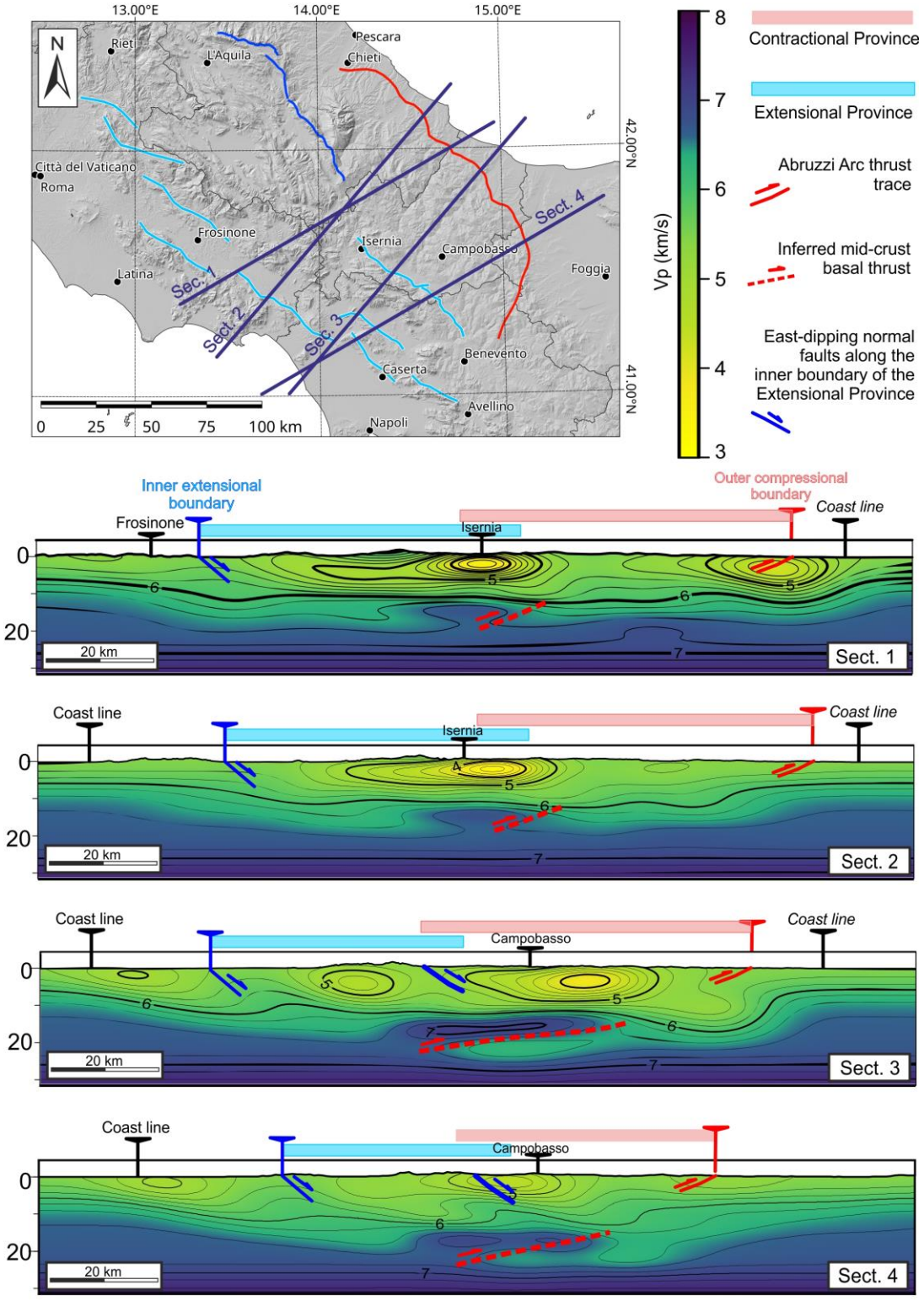
13.00°E
14.00°E
15.00°E
42.00°N
41.00°N
N
Rieti
L'Aquila
Pescara
Chieti
Città del Vaticano
Roma
Frosinone
Isernia
Campobasso
Foggia
Latina
Benevento
Caserta
Avellino
Napoli
Sect. 1
Sect. 2
Sect. 3
Sect. 4
0 25 50 75 100 km
Vp (km/s)
8
7
6
5
4
3
Contractional Province
Extensional Province
Abruzzi Arc thrust trace
Inferred mid-crust basal thrust
East-dipping normal faults along the inner boundary of the Extensional Province
Inner extensional boundary
Outer compressional boundary
Coast line
Frosinone
Isernia
0
20
20 km
Sect. 1
Coast line
Isernia
Coast line
Sect. 2
Coast line
Campobasso
Coast line
Sect. 3
Coast line
Campobasso
Sect. 4

Figure ~~5~~6. Tomographic section views. a) Location map with the ~~grid of~~ cross-sections of the tomographic Vp model shown below. ~~on which the approximate attitude of the main structural domain boundaries has been drawn. Purple lines on the upper left panel represent the traces of the four sections.~~ The light blue and light red bars above all the cross-sections represent the boundaries of the Apennine extensional province and the external compressional province, respectively, as indicated in the Fig. 1b. Geometry of the inferred mid-crust basal thrust is retrieved from the velocity inversion.

~~4~~5.2 Instrumental seismicity and new focal mechanism solutions

During the instrumental period, spanning 1981 to 2018, the seismotectonic domains within the study area (extensional, contractional, and strike-slip from west to east) ~~(Figs. 1, 2, S29~~15a) are characterized by low seismicity rates (Figs. 1, 2, S29a). The recorded seismicity predominantly consists of swarms and moderate seismic sequences (M_L 0.0–5.4). The completeness magnitude of the Italian seismic catalogues has varied over time (Amato and Mele, 2008; Schorlemmer et al., 2010), with a notable decrease observed only after 2009 (from approximately M_L 2.0 to M_L 1.4) (Figs. S29~~15~~b, c).

Focusing on the northern Abruzzi Arc basal thrust, the sector west of the front displays a seismic gap, as evidenced by the epicentral distributions in the Italian catalogue (CLASS, Latorre et al., 2023; inset in Fig. 3c). However, southwest of the Maiella thrust front (dashed grey line in Fig. 3a,c), our analysis of relocated seismicity from Romano et al., (2013) reveals compressional activity ~~in~~ especially in 2009 ~~and 2018, occurring at depths between 8 and 18 km.~~

The 2009 sequence was concentrated along an antithetic structure of the Abruzzi Arc basal thrust (red dots in Fig~~s~~. 3~~b,~~ d), representing the most energetic cluster (maximum M_L 3.8). The corresponding hypocentres and focal mechanisms delineate an eastward-dipping back thrust splaying from the basal thrust between 8 and 11 km depth. ~~In contrast, the 2018 activity involved the down-dip portion of the same thrust system and includes a westward-deepening microseismic volume at 15–18 km depth highlighted by the CLASS epicentral distribution (green contours in Figs. 3b and d).~~ New focal mechanisms (1-7), indicating reverse-oblique kinematics, support this finding, with P-axes rotating from SW-NE to E-W southward (Figs. 3c and ~~S11~~S13).

Earthquakes recorded, such as San Giuliano 2002 (M_W 5.7) and Montecifone 2018 (M_W 5.1) (Fig. 3c) are relatively energetic but do not belong to the compressional province. They are associated with the foreland strike-slip domain. These events activated E–W trending, sub-vertical faults with right-lateral kinematics, located within the footwall of the Abruzzi Arc basal thrust, at depths ranging from 10 to 20 km (green dots in Fig. 3d).

The 2002 sequence consisted of two mainshocks of equal magnitude (Mw 5.7) occurring within 20 hours of each other (Chiarabba et al., 2005a). The aftershock distribution reveals a westward-deepening seismogenic volume (Fig. 3d), which may indicate that the Abruzzi Arc basal thrust acted as a structural barrier to the upward propagation of rupture.

In the southern sector of the Abruzzi Arc basal thrust, near the surface boundary with the extensional domain, the 1986 (Md 4.1) and 1997 (Md 4.1) normal faulting earthquakes occurred at the tip of the Bojano east-dipping normal fault system (Milano, 2023). The 2016 event (M_L4.1) involved an east-dipping low-angle splay of the same system (Figs. 3c, S3).

45.3 Structural Model and Crustal Architecture of the Abruzzi Arc basal thrust

45.3.1 Surface Geometry and Arc Hierarchy

The geological data compiled and analysed for this study provided the basis for a new structural map of the Abruzzi Arc basal thrust, which include the traces of both outcropping fold-and-thrust structures and inferred buried thrusts (Fig. 3). The thrust system extends for approximately 170 km along strike from NW–SE to N–S and then to NNE–SSW, forming a broad eastward-convex arcuate geometry.

The overall shape and extent of the Abruzzi Arc basal thrust closely match those of the Ferrara and Emilia third-order arcs within the Italian Outer Thrust System (OTS) (Figs. 1a, S1), consistent with the hierarchical classification proposed by Caputo and Tarabusi (2016) and later adopted by Tibaldi et al. (2023).

Along strike, the Abruzzi Arc basal thrust is segmented into three fourth-order arc segments, each approximately 40 to 50 km long: Abruzzo Citeriore, Frentani, and Daunia (Fig. 3a).

The thrust system includes two main structural alignments. The internal alignment, located in the Apennine foothills, is characterized by outcropping fold-and-thrust structures developed during the Late Pliocene to Early Pleistocene, which involve the sedimentary cover of the Apulian foreland platform. The external alignment, largely buried, is inferred through the analysis of topographic relief and fluvial network patterns (Ferrarini et al., 2021a).

45.3.2 Crustal-Scale Geometry and Structural Style

The crustal-scale geometry and structural style of the Abruzzi Arc basal thrust were mainly interpreted from three regional cross-sections (Figs. 3 and ~~S12~~S14): the near-vertical CROP 11 deep seismic profile across the Abruzzo Citeriore sector (Di Luzio et al., 2009; Patacca et al., 2008), a crustal transect across the Majella Massif and the Abruzzo Citeriore segment (Ferrarini et al., 2021a), and balanced cross-sections across the Matese Massif and the Frentani Arc (Butler et al., 2004). These sections consistently show that the arc involves the Apulian foreland's sedimentary crust, overlain by thin allochthonous thrust sheets belonging to the Sannio-Molise units, and underlain by the crystalline basement. The basal thrust penetrates to depths of at least 12 to 15 km and is associated with several synthetic and antithetic splays developed at both upper- and mid-crustal levels. Its along-dip geometry is characterized by flat and ramp segments, reflecting an overall thick-skinned tectonic style. A horizontal displacement of approximately 4 to 5 km, estimated from balancing techniques across the Frentani Arc (Butler et al., 2004), is consistent with the current position of the Abruzzi frontal thrust relative to the deepest mapped Plio-Pleistocene deposits in its footwall. These deposits are represented by the depth contours of the Pliocene base in the Structural Model of Italy at 1:500.000 scale (Bigi et al., 1992).

45.4 3D Conceptual 3D Faul Model

45.4.1 The Abruzzi Arc basal thrust

We constructed a three-dimensional conceptual model of the Abruzzi Arc basal thrust by integrating the geological and geophysical constraints described above with the tomographic data from this study. The resulting non-planar surface extends for approximately 170 km along strike, with an average dip angle of ~22°, and reaches depths of up to 24 km (Fig. 6c7c).

The input data used for model construction are illustrated in Figure 6a7a. Green lines represent thrust geometries derived from geological cross-sections and structural transects, while purple lines highlight selected profiles that provide the clearest tomographic constraints. Figure 67b shows the 3D view of two iso-surfaces corresponding to P-wave velocities of 6.6 km/s, delineating the upper and lower boundaries of a mid-crustal low-velocity zone, interpreted as an inversion structure due to crustal doubling.

At shallow depths, from 0 to 5 km, the geometry of the basal thrust is primarily constrained by surface and near-surface geological data across the Abruzzi Arc basal thrust and was constructed by planar extrusion of the frontal thrust traces.

At mid-crustal depths, between approximately 16 and 24 km, beneath the Frentani and Daunia segments, and farther north beneath the Abruzzo Citeriore, the geometry of the basal thrust was inferred from the interface between high- and underlying low-velocity zones identified in the tomographic model (Fig. 6). The resulting tomography-derived fault patch extends for about 100 km along strike and dips south-west with an average angle of about 15°, as shown by the polygon in Figure 7c.

At depths between 5 and 16 km, the geometry of the basal thrust was built by interpolating the shallow and deep surfaces.

The model is locally constrained by seismicity and new focal mechanisms, for example, by the geometry and position of a back-thrust and the deeper portion of the thrust identified in the Frentani segment, located between 8 and 18 km depth (Fig. 3d). Additional constraints come from the location of strike-slip faults in the Adriatic foreland and the upper tip lines of the reconstructed 3D fault patch of normal faults (next section).

45.4.2 The extensional and strike-slip structures

To integrate the conceptual model of the Abruzzi Arc basal thrust into a broader seismotectonic framework, we also constructed a simplified 3D model of the major neighbouring structures (Fig. 67c). These include the west- and east-dipping normal faults located along the western and eastern boundaries of the extensional province, as well as the strike-slip and normal-oblique faults across the outermost tectonic province.

The traces of the normal faults shown in the map of Figure 3 were planarly extruded along dip to a depth of 12 km. A fixed dip angle of 60° was adopted for the west-dipping normal faults from Gran Sasso to Mt. Cappucciata, Morrone, and Porrara (n. 9 to 12 in Figs. 76c and S3). A dip angle of 45° was assumed for the east-dipping normal faults that dissect the Latium-Northern Campania carbonate massifs of the Late Miocene–Early Pliocene fold-and-thrust belt, including the Simbruini, Ernici, Lepini, Ausoni–Aurunci, Mt. Taburno, Caserta, and Mt. Avella ranges (numbered 1 to 8 in Fig. 67c), and for the east-dipping Boiano and Sepino faults (numbered 13 and 14 in Figs. 67c and S3).

Similarly, the oblique strike-slip faults cropping out in the western Gargano Promontory area, including the well-known Apricena Fault (Patacca and Scandone, 2004) (number 15 in Figs. ~~6~~7c and S3), were planarly extruded to a depth of 12 km, assuming a constant dip angle of 80°.

The 3D geometry of the blind, steep, north-dipping, right-lateral seismogenic patches responsible for the 2002 San Giuliano (Mw 5.7) and 2018 Montecilfone (Mw 5.1) earthquake sequences (Di Luccio et al., 2005) and for a few other minor sequences (Trionfera et al., 2019), was reconstructed using Inverse Distance Weighting (IDW) interpolation of seismicity (Lavecchia et al., 2025). These patches (numbered 16 in Fig. ~~6~~7c) are located at depths between ~10 and 25 km and show a progressive westward-deepening of the uppermost seismogenic depth, supporting the hypothesis that the upward propagation is inhibited by the basal thrust, which likely acts as a mechanical barrier.

Such a structural configuration, in which strike-slip faults remain confined beneath a low-angle basal thrust that prevents their upward propagation, has been recognized in several sectors of the Italian Outer Thrust System (OTS), including the northern (de Nardis et al., 2024), central, and southern Apennines (Adinolfi et al., 2015; Boncio et al., 2007), as well as Sicily (Lavecchia et al., 2007; Visini et al., 2009).

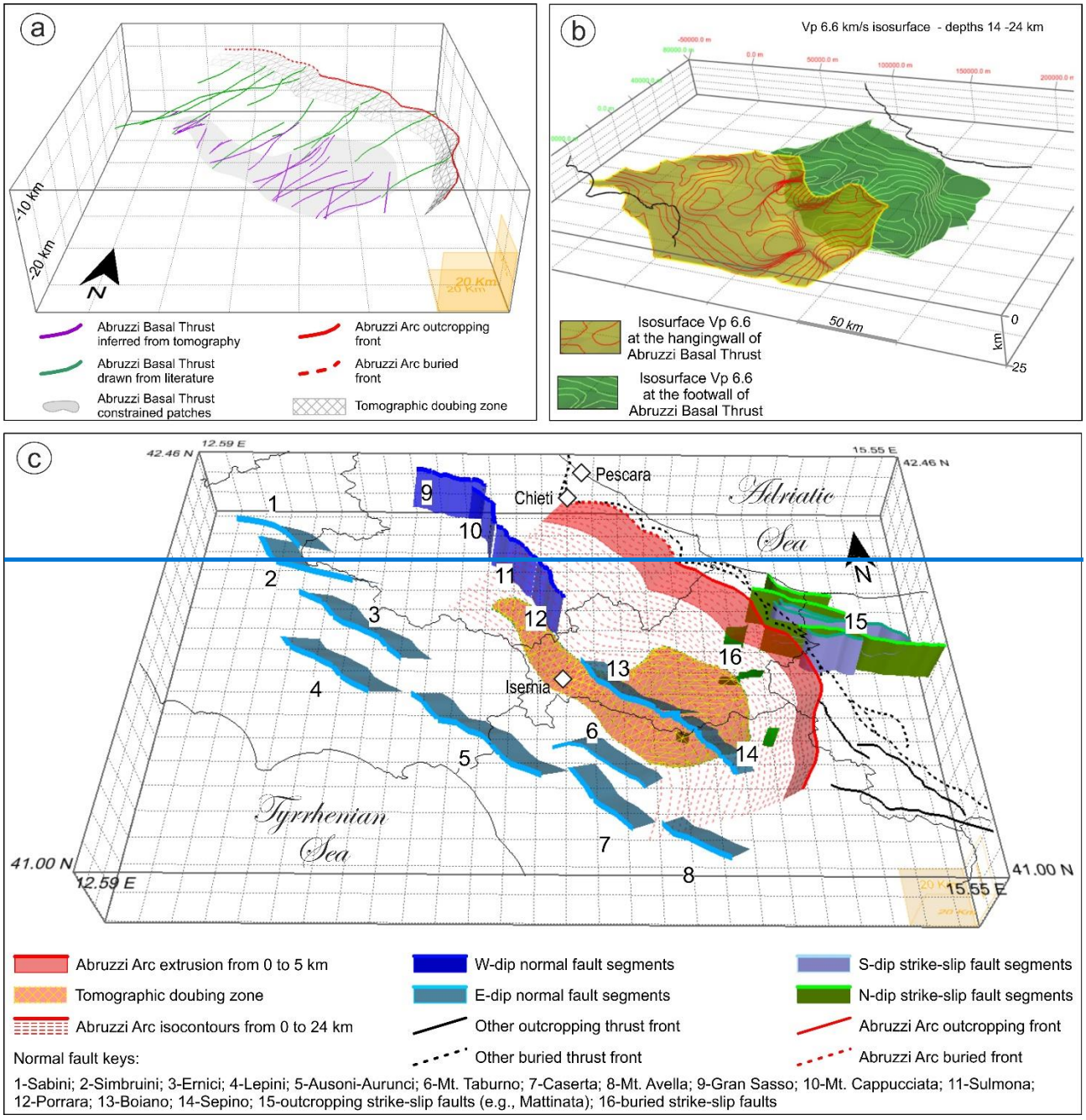
a
-10 km
-20 km
N
20 Km
Abruzzi Basal Thrust inferred from tomography
Abruzzi Basal Thrust drawn from literature
Abruzzi Basal Thrust constrained patches
Abruzzi Arc outcropping front
Abruzzi Arc buried front
Tomographic doubing zone
b
Vp 6.6 km/s isosurface - depths 14 -24 km
50 km
0
km
25
Isosurface Vp 6.6 at the hangingwall of Abruzzi Basal Thrust
Isosurface Vp 6.6 at the footwall of Abruzzi Basal Thrust
c
42.46 N
12.59 E
15.55 E
Pescara
Chieti
Adriatic Sea
N
Isernia
Tyrrhenian Sea
41.00 N
1
2
3
4
5
6
7
8
9
10
11
12
13
14
15
16
Abruzzi Arc extrusion from 0 to 5 km
Tomographic doubing zone
Abruzzi Arc isocontours from 0 to 24 km
Normal fault keys:
W-dip normal fault segments
E-dip normal fault segments
Other outcropping thrust front
Other buried thrust front
S-dip strike-slip fault segments
N-dip strike-slip fault segments
Abruzzi Arc outcropping front
Abruzzi Arc buried front
1-Sabini; 2-Simbruini; 3-Ernici; 4-Lepini; 5-Ausoni-Aurunci; 6-Mt. Taburno; 7-Caserta; 8-Mt. Avella; 9-Gran Sasso; 10-Mt. Cappucciata; 11-Sulmona; 12-Porrara; 13-Boiano; 14-Sepino; 15-outcropping strike-slip faults (e.g., Mattinata); 16-buried strike-slip faults

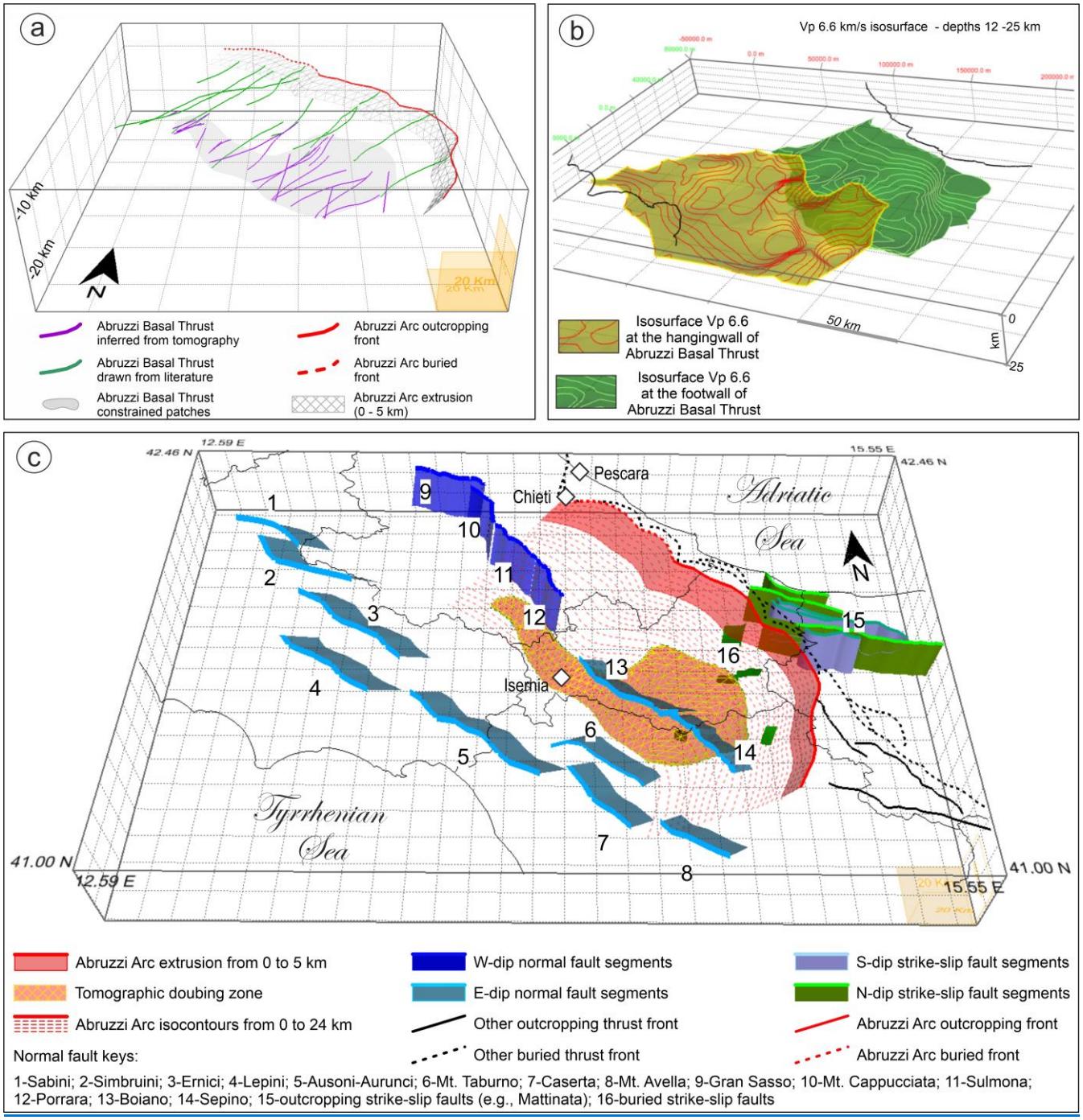

Figure 6~~7~~. 3D fault model within the boundaries of the tomographic study area. a) 3D view of the Abruzzi Arc basal thrust representing the constrained (grey areas) and interpolated (white zones) fault surface. The purple lines represent the along-dip traces of the Abruzzi Arc basal thrust inferred from seismic tomography, while the green ones are those from geological and geophysical sections (see Fig. S1~~2~~4). b) Iso-surface corresponding to Vp 6.6 km/s. c) Whole 3D conceptual model representing the Abruzzi Arc basal thrust (red surface), and the main geological structures belonging to the extensional (n. 1 to 14) and strike-slip

domains (n. 15-16). The yellow mesh represents the area where a crustal doubling across the Abruzzi Arc basal thrust is imaged by seismic tomography.

~~5~~ 6 Discussion

The seismotectonic characterization of the Abruzzi Arc basal thrust is a scientific challenge due to its location in the transition zone between the Central and the Southern OTS of Italy, the complex geometry, low seismic activity, and never-addressed 3D structural style. In this study, we perform a travel time tomography to gain insights into the crustal structure of this complex sector of the Apennines. The optimal distribution of earthquake hypocentres at the hanging wall and footwall of the Abruzzi Arc basal thrust, together with the increased number of seismic stations deployed after 2009 (Amato and Mele, 2008; Schorlemmer et al., 2010), allows us to obtain the first seismic images showing features compatible with a crustal doubling across the Abruzzi thrust system at mid-crust depths. Our results are included in a 3D conceptual model of the tectonic setting of this sector of the Apennine, which clarifies the relationship among the three tectonic provinces coexisting in this area.

~~5~~6.1 Structural Style

The structural style of thrust tectonics in the Apennines (Italy) has been extensively but contrastingly described in the literature (e.g., Bally et al., 1986; Boccaletti et al., 2005; Butler et al., 2004; Casero et al., 1991; Doglioni, 1987; Lavecchia et al., 1994; Mazzoli et al., 2000; Mazzotti et al., 2000; Noguera and Rea, 2000; Scrocca et al., 2005; Speranza and Chiappini, 2002; Steckler et al., 2008). The geometric elements that characterize the deformation style as thick (deformation affecting both the sedimentary cover and the underlying crystalline basement rocks) or thin-skinned (deformation primarily confined to the upper sedimentary layers above a detachment fault, without significantly impacting the underlying basement rocks) are not always univocal, so that both tectonic models are often considered valid options. Applying these interpretative models is critical to understanding the geodynamic context, as they directly affect the estimate of shortening rates.

In the early 2000s, Tozer et al. (2002), and later Boccaletti et al. (2005), proposed a thick-skinned deformation style for the southern-central Apennines, based on estimates of low shortening rates. At the same time, Calabrò et al. (2003) also suggest a thin-skinned deformation based on magnetotelluric and geological survey data. Geophysical data cannot solve the problem due to a usual contradiction with the geological information, with both interpretations remaining admissible (e.g., Steckler et al., 2008). Indeed, Butler et al. (2004), and Mazzoli et al. (2000) justify the previous interpretations' inconsistency by proposing a mixed-type tectonic model. They hypothesize a temporal and spatial variability in deformation styles throughout the Apennines, ranging from thin-skinned to thick-skinned.

Focusing exclusively on the last phase of the eastward propagating compressional phase, which began in the Late Pliocene and is widely accepted to have lasted at least until the Early Pleistocene, there is general agreement on the predominance of a

thick-skinned tectonic style (Butler et al., 2004, and references therein). In the central-southern Apennines, this phase involved the Apulian foreland's sedimentary crust, the overlying thin thrust allochthonous sheets of the Sannio-Molise units, and the underlying crystalline basement. Following this setting, during the last phase, the gently westward-dipping Adriatic foreland was likely overthrust through the Abruzzi Arc basal thrust onto the Late Pliocene foredeep deposits. Such a setting is well fitted by the basal thrust penetrated to depths of 24 km in the inner part of the chain (Figs. 6~~5~~, ~~6~~7, and ~~7~~8)~~,~~ and showing continuity and agreement with the compressive structure reconstructed by Chiarabba et al. (2010).

The reconstructed 3D geometry of the Abruzzi Arc basal thrust well correlates in size, shape, and structural style with those proposed for the third-order arcs of the Padan-Adriatic frontal thrust system, such as the Monferrato Arc (Turrini et al., 2014), the Emilia Arc (Tibaldi et al., 2023), the Ferrara Arc (Improta et al., 2023), as well as the Adriatic Arc.

Considering the new findings presented in this paper, particularly the arcuate shape and the lower crust doubling imaged by tomography, we propose that the Abruzzi Arc basal thrust might represent the southernmost element of a larger crust-scale frontal thrust.

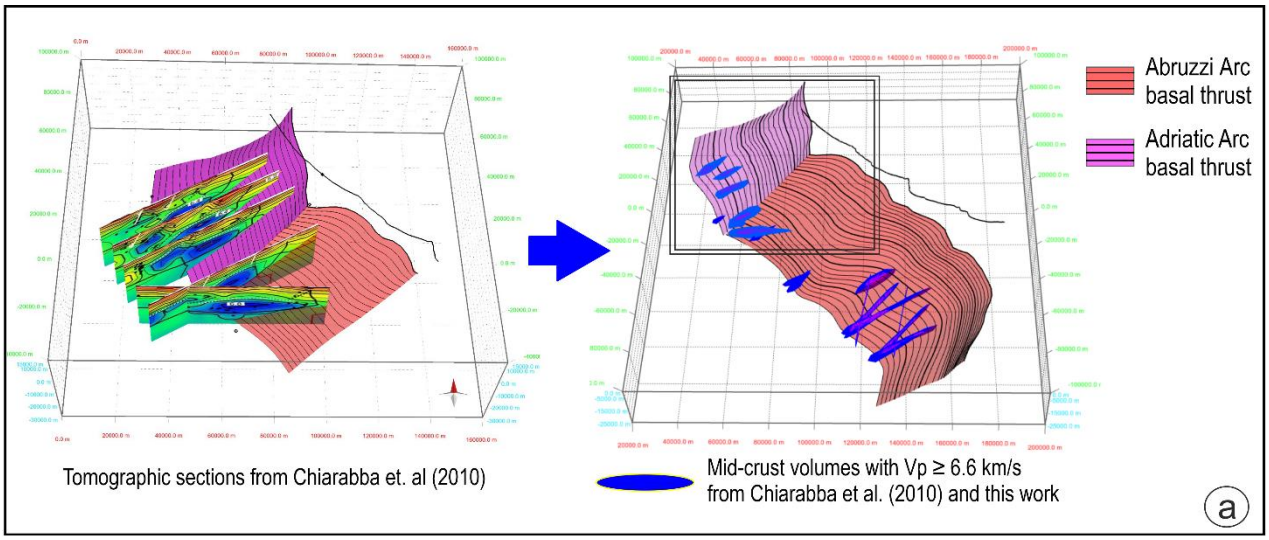

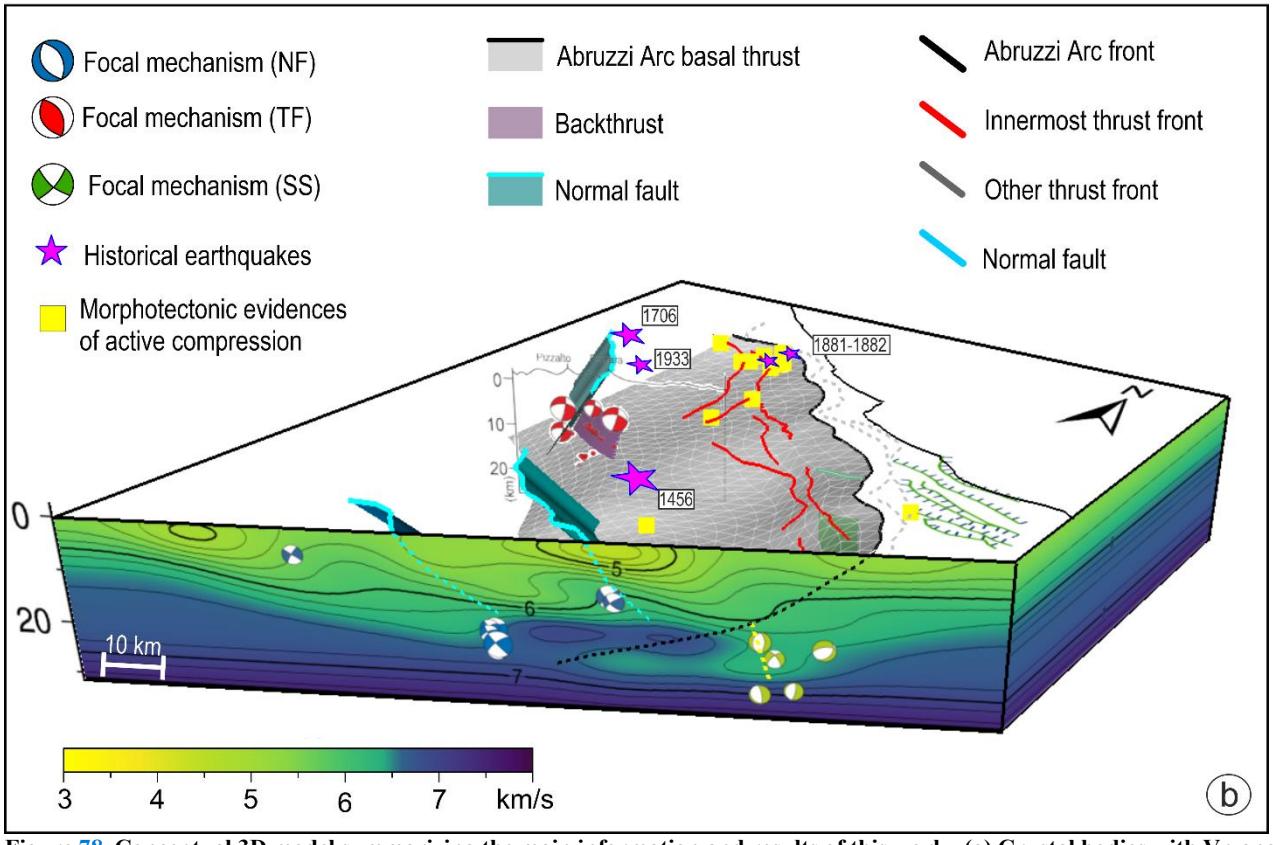

Figure 7[8]. Conceptual 3D model summarizing the main information and results of this work. (a) Crustal bodies with Vp anomalies ≥ 6.6 km/s redrawn from Chiarabba et al. (2010) at the hanging wall of the Adriatic Arc basal thrust and from this study at the hanging wall of the Abruzzi Arc basal thrust. (b) Main conceptual fault surfaces as in fig 6[7]c, the epicentres of historical earthquakes (purple stars) and the sites where the morphological evidence of active compression has been found (yellow squares) are reported. The surface of a minor back thrust (Figs 3b, d) is shown by seismicity and focal mechanisms. Focal mechanisms from the literature are also overlapped with the Vp tomographic sections.

56.2 Activity vs inactivity

As observed by instrumental seismic catalogues (International Seismological Center, 2024), along some compressive segments of the Circum-Mediterranean fold and thrust belt, the background seismicity and overall seismicity rates are low. For instance, the recent 2023 Morocco seismic sequence, with a mainshock of Mw 6.8, occurred in the western High Atlas, an area with low seismicity rates (Onana et al., 2011; Sébrier et al., 2006).

Over the last forty years, the Italian instrumental seismicity highlights that the seismicity rates associated with the compressional domain vary from very low to low (Taroni and Carafa, 2023). The so-called Emilia earthquake in 2012 (M_W 6.0) occurred unexpectedly (e.g., Govoni et al., 2014; Improta et al., 2023; Lavecchia et al., 2015), as well as the Belice earthquake in Sicily in 1968 (M_W 6.0) (Orecchio et al., 2021), activating thrust zones that were previously silent from a seismic perspective.

In this context, the Abruzzi Arc basal thrust appears aseismic when considering instrumental seismicity from 1981 to the present (Figs. 1b, 3c), except for minor compressional activity (maximum M_L 3.8) documented in this study. This activity occurred in 2009 and 2018 at depths ranging from 8 to 18 km and is closely associated with the deeper portions of the Abruzzo Citeriore thrust segment and its back thrust (Fig. 3b, d).

By contrast, the earthquake/fault association of some historical events is still largely debated. Close to the outer boundary of the extensional province, at the hanging wall of the Abruzzi Arc basal thrust, some destructive earthquakes have occurred such as 1706 (M_W 6.8), 1933 (M_W 6.0), 1881 (M_W 5.6), 5 December 1456, (M_W 7.2), and a few moderate ones (1882, M_W 5.2, 1905, M_W 5.2) (CPTI15v4, Rovida et al., 2020, 2022) (Figs. 2a, ~~b,~~ 78, S2).

Paleoseismological and archaeological studies (Ceccaroni et al., 2009; Galadini and Galli, 2000; Galli et al., 2015; Puliti et al., 2025) associated the 1706 event with the extensional domain, while de Nardis et al. (2008), by macroseismic field inversion, tentatively associated this earthquake and the 1933 one with the mid-crust portion of the Abruzzi Arc basal thrust, in correspondence of the Abruzzo Citeriore segment. The Italian Database of Seismogenic Sources (DISS Working Group, 2021) reports such an interpretation. Galli and Pallone (2019), by revising the macroseismic field of the 1933 earthquake, associated this event with a back thrust corresponding to the one we unveiled with the seismicity distribution and new focal mechanisms in this study. Similarly, Volatili et al. (2025) advanced the hypothesis that 1706 is associated with a back thrust of the Abruzzi thrust system.

The tomographic Abruzzi doubling zone identified in this paper (Figs. 56-7) also partially underlies the macroseismic field of the 1456 destructive sequence (Fig. S2a), which consisted of multiple events ~~(Fig.2b")~~. The most widely accepted interpretations associate the 1456 sequence with E–W trending transcurrent faults located in the footwall of the Abruzzi Arc basal thrust (DISS Working Group, 2021; Fracassi and Valensise, 2007). However, a recent study by Amato et al. (2025), based on a multi-scale and multidisciplinary approach, links this sequence to the extensional domain. Given the unclear and complex context, an association of this earthquake with the Abruzzi thrust system cannot be ruled out. In our opinion, further investigation is needed to resolve these contrasting interpretations.

In any case, in support of the hypothesis of active compression of the Abruzzi thrust system, morphotectonic studies have shown the activation of the compressive structures since at least the Middle Pleistocene, along the coastal sector of the Abruzzo Citeriore and its inner foothill sector (e.g., Casoli and Bomba structural high, Pomposo and Pizzi, 2009; Racano et al., 2020). Ferrarini et al. (2021a), through analyses of topography, fluvial networks, and landscape evolution in the northern portion of the Abruzzi Arc basal thrust, identified patterns of anomalies supporting tectonic uplift and shortening (see yellow ~~dots~~squares in Fig.8~~7~~). The same authors did not find morphotectonic data indicating active deformation across the southernmost portion of the thrust. Furthermore, through seismic line interpretations, they highlighted Middle Pleistocene to Holocene compression in the Adriatic Arc's southern portion, along the Abruzzi Arc basal thrust northward prosecution.

The slow deformation rate, the possibility of long recurrence intervals, and the absence of earthquakes along the Abruzzi thrust system do not rule out potential future seismic activity. It is also important to note that the earthquake-thrust association, observed in other third-order arcs of the Padan-Adriatic Arc, indicates moderate compressional seismicity occurring along the basal thrust and its splays, both at upper crustal depths and in the mid-to-lower crust, as the July 2002 Modena earthquake - M_W 4.2, the 2003 Monghidoro earthquake - M_W 5.3 (Piccinini et al., 2006), the 2007–2008 Langhirano earthquakes, M_W 5.5, and the 2024 Langhirano earthquake, M_W 4.2 (CLASS, Latorre et al., 2023).

Concluding, while some recent studies (e.g., Lanari et al., 2023), based on integrated surface and deep-process analyses, consider the Abruzzi area to be inactive, the data and interpretations presented in this paper do not exclude the possibility of its activity, comparable to that of other arcs of the Italian OTS. If confirmed, this hypothesis would have significant implications not only for seismic potential assessment but also for the understanding of regional geodynamics.

~~6~~ 7 Final remarks

This study provides new insights into the 3D structural complexity of the Central-Southern Apennines segment of the Outer Thrust System through a multidisciplinary approach that integrates seismic tomography, instrumental seismicity, focal mechanism solutions, and geological data. A newly structural map allows us to define the system as an eastward convex arc, the Abruzzi Arc basal thrust, which extends along strike for ~170 km and is articulated into three minor order arcs (Abruzzo Citeriore, Frentani, and Daunia). The geometry of the Abruzzi Arc basal thrust well aligns with that of the third-order arcs of the Padan-Adriatic belt, supporting the hierarchical framework of thrust tectonics along the OTS of Italy (Caputo and Tarabusi, 2016; Petricca et al., 2019).

Seismic tomography reveals a mid-crustal velocity inversion (14–24 km depth) beneath the Frentani and Daunia arcs, interpreted as evidence of crustal doubling and consistent with thick-skinned thrust deformation. Analogous patterns are observed in southern Marche and northern Abruzzo (Chiarabba et al., 2010). These findings point to a classical overthrust architecture and align with the structural style of the adjacent Northern and Central OTS sectors. These findings contribute to a 3D conceptual model of the tectonic setting in central-southern Italy, capturing the basal shear zone of the Abruzzi fold-and-

thrust system at depth, and showing the possible relationship between extensional, contractional, and strike-slip provinces here coexisting.

The activity and seismogenic role of the Abruzzi Arc basal thrust and its splays remain a topic of debate. While instrumental seismicity shows only modest and localized minor compressional activity at mid-crust depths, some major historical records, such as, for example, the 1706 earthquake, if associated with the thrust structure, could imply a capability of releasing strong earthquakes, maybe with long recurrence intervals. Morphotectonic studies further corroborate ongoing compressional deformation in segments like the Abruzzo Citeriore thrust, evidenced by uplift and fluvial network anomalies.

In conclusion, in this study, tomographic images and geological data enhance the understanding of the Abruzzi Arc basal thrust three-dimensional structural style and regional seismotectonic behaviour.

We offer a new framework for future investigation about the overall OTS of Italy, its seismic potential, and the broader geodynamic implications. In particular, the conceptual model of the Abruzzi thrust system might be functional for a new generation of 3D seismic hazard models applicable to complex seismotectonic domains (Pandolfi et al., 2023, 2024).

~~Appendix A~~

~~Setting of parameters and synthetic tests for the travel time tomography~~

~~The inversion model setting is the most challenging and time-consuming phase of the tomographic process. We find the best grid node spacing to be half the average distance of the nearest station as the horizontal spacing and half the standard deviation (σ) of the earthquake depth distribution as the vertical spacing. This combination gives the lower residuals root mean square (RMS) in the direct phase of the process. Similarly, we select 12 iterations for evaluating when the residuals stop decreasing significantly, which indicates a convergence to the absolute minimum. Finally, we establish damping and smoothing parameters based on the trade-off curves.~~

~~The next step involves testing the reliability of the results based on synthetic models. The checkerboards have variable sizes corresponding to twice the propagation grid spacing (10 * 10 * 4 km), three times the propagation grid spacing (15 * 15 * 6 km), and four times the same value (20 * 20 * 8 km). Random noise with a priori model covariance is added to the synthetic data; the models are reconstructed without relocating the seismic events to test the source-receiver distribution. Results shown in Fig. S9 exhibit an excellent restoration of the synthetic model in the belt area, especially for the largest anomalies (about 20 km wide and 8 km thick). Relevant issues can be found in reconstructing the intermediate sizes of the checkerboard anomalies, for which the synthetic features can only be recognized under the Apennine chain. Fig. S9 also reveals a higher sensibility of S-waves in detecting the sharp separation of positive and negative anomalies in the checkerboard model than P-waves, whose model appears smoother. The last two synthetic tests involve spikes north of Isernia and Campobasso towns (Fig. S10). Here, the results depict a strong velocity inversion extending about 30 * 30 * 4 km between 16 and 24 km of depth. We imposed a first spike reproducing the anomaly (high velocity over low velocity zone), and an inverted one (low velocity over high velocity volume): location and details are shown in Fig. S10, where the anomalies are crossed with two perpendicular vertical~~

~~sections spanning the entire model volume. Both synthetic spikes can be reconstructed using the FMTOMO code, suggesting that the anomaly is stable and reliable.~~

dReferences

Adinolfi, G. M., De Matteis, R., Orefice, A., Festa, G., Zollo, A., de Nardis, R., and Lavecchia, G.: The September 27, 2012, ML 4.1, Benevento earthquake: A case of strike-slip faulting in Southern Apennines (Italy), Tectonophysics, 660, 35–46, https://doi.org/10.1016/j.tecto.2015.06.036, 2015.

Amato, A. and Mele, F. M.: Performance of the INGV National Seismic Network from 1997 to 2007, Performance of the INGV National Seismic Network from 1997 to 2007, Annals of Geophysics, 15, 2008.

Amato, V., Ciarcia, S., Galli, P., Cicchella, D., Galderisi, A., Monaco, L., Fernandez, G., Isaia, R., Nomade, S., Pereira, A., and Giaccio, B.: Unveiling the hidden source of major historical earthquakes: A multi-scale, trans-disciplinary approach to the 1456 and 1688 Sannio earthquakes (Mw 7.0, southern Italian Apennines), Quaternary Science Reviews, 356, 109282, https://doi.org/10.1016/j.quascirev.2025.109282, 2025.

Argnani, A., Rovere, M., and Bonazzi, C.: Tectonics of the Mattinata fault, offshore south Gargano (southern Adriatic Sea, Italy): Implications for active deformation and seismotectonics in the foreland of the Southern Apennines, Geological Society of America Bulletin, 121, 1421–1440, https://doi.org/10.1130/B26326.1, 2009.

Bally, A. W., Burbi, L., Cooper, C., and Ghelardoni, R.: Balanced sections and seismic reflection profiles across the central apennines, Mem. Soc. Geol. It., 35, 257–310, 1986.

Battistelli, M., Ferrarini, F., Bucci, F., Santangelo, M., Cardinali, M., Merryman Boncori, J. P., Cirillo, D., Carafa, M. M. C., and Brozzetti, F.: Bridging the Gap Between Active Faulting and Deformation Across Normal-Fault Systems in the Central–Southern Apennines (Italy): Multi-Scale and Multi-Source Data Analysis, Remote Sensing, 17, 2491, https://doi.org/10.3390/rs17142491, 2025.

Bell, K., Lavecchia, G., and Rosatelli, G.: Cenozoic Italian magmatism – Isotope constraints for possible plume-related activity, Journal of South American Earth Sciences, 41, 22–40, https://doi.org/10.1016/j.jsames.2012.10.005, 2013.

Bigi, G., Coli, M., Cosentino, D., Parotto, M., Praturlon, A., Sartori, R., Scandone, P., and Turco, E.: Structural Model of Italy scale 1:500.000, sheet 4. C.N.R., Progetto Finalizzato Geodinamica, SELCA Firenze., Progetto Finalizzato Geodinamica, SELCA Firenze., 1992.

Bisio, L., Di Giovambattista, R., Milano, G., and Chiarabba, C.: Three-dimensional earthquake locations and upper crustal structure of the Sannio-Matese region (southern Italy), Tectonophysics, 385, 121–136, https://doi.org/10.1016/j.tecto.2004.01.007, 2004.

Boccaletti, M., Calamita, F., and Viandante, M. G.: La Neo-Catena litosferica appenninica nata a partire dal Pliocene inferiore come espressione della convergenza Africa-Europa, Bollettino della Società Geologica Italiana, 124, 87–105, 2005.

Bollinger, L., Klinger, Y., Forman, S. L., Chimed, O., Bayasgalan, A., Munkhuu, U., Davaasuren, G., Dolgorsuren, T., Enkhee, B., and Sodnomsambuu, D.: OPEN 25,000 Years long seismic cycle in a slow deforming continental region of Mongolia, Scientific Reports, 2021.

Boncio, P., Mancini, T., Lavecchia, G., and Selvaggi, G.: Seismotectonics of strike–slip earthquakes within the deep crust of southern Italy: Geometry, kinematics, stress field and crustal rheology of the Potenza 1990–1991 seismic sequences (Mmax 5.7), Tectonophysics, 445, 281–300, https://doi.org/10.1016/j.tecto.2007.08.016, 2007.

Brozzetti, F.: The Campania-Lucania Extensional Fault System, southern Italy: A suggestion for a uniform model of active extension in the Italian Apennines, Tectonics, 30, 2010TC002794, https://doi.org/10.1029/2010TC002794, 2011.

Brozzetti, F., Cirillo, D., de Nardis, R., Cardinali, M., Lavecchia, G., Orecchio, B., Presti, D., and Totaro, C.: Newly identified active faults in the Pollino seismic gap, southern Italy, and their seismotectonic significance, Journal of Structural Geology, 94, 13–31, https://doi.org/10.1016/j.jsg.2016.10.005, 2017.

Butler, R. W. H., Mazzoli, S., Corrado, S., De Donatis, M., Di Bucci, D., Gambini, R., Naso, G., Nicolai, C., Scrocca, D., Shiner, P., and Zucconi, V.: Applying Thick-skinned Tectonic Models to the Apennine Thrust Belt of Italy — Limitations and Implications, in: Thrust Tectonics and Hydrocarbon Systems, American Association of Petroleum Geologists, 647–667, https://doi.org/10.1306/M82813C34, 2004.

Calabrò, R. A., Corrado, S., Di Bucci, D., Robustini, P., and Tornaghi, M.: Thin-skinned vs. thick-skinned tectonics in the Matese Massif, Central–Southern Apennines (Italy), Tectonophysics, 377, 269–297, https://doi.org/10.1016/j.tecto.2003.09.010, 2003.

Caputo, R. and Tarabusi, G.: Il complesso sistema di sorgenti sismogeniche nell'area ferrarese e i loro effetti nella storia., 2016.

Carafa, M. M. C. and Bird, P.: Improving deformation models by discounting transient signals in geodetic data: 2. Geodetic data, stress directions, and long-term strain rates in Italy: DISCOUNTING TRANSIENT SIGNALS: 2. ITALY, J. Geophys. Res. Solid Earth, 121, 5557–5575, https://doi.org/10.1002/2016JB013038, 2016.

Casero, P., Roure, F., and Vially, R.: Tectonic framework and petroleum potential of the Southern Apennines, in: Generation, accumulation, and production of Europe's hydrocarbons: Special Publication of the European Association of Petroleum Geoscientists, vol. 1, Oxford University Press, Oxford, 381–387, 1991.

Ceccaroni, E., Ameri, G., Gómez Capera, A. A., and Galadini, F.: The 2nd century AD earthquake in central Italy: archaeoseismological data and seismotectonic implications, Nat Hazards, 50, 335–359, https://doi.org/10.1007/s11069-009-9343-x, 2009.

Cheloni, D., Famiglietti, N. A., Tolomei, C., Caputo, R., and Vicari, A.: The 8 September 2023, M_W 6.8, Morocco Earthquake: A Deep Transpressive Faulting Along the Active High Atlas Mountain Belt, Geophysical Research Letters, 51, e2023GL106992, https://doi.org/10.1029/2023GL106992, 2024.

Chiarabba, C., Jovane, L., and DiStefano, R.: A new view of Italian seismicity using 20 years of instrumental recordings, Tectonophysics, 395, 251–268, https://doi.org/10.1016/j.tecto.2004.09.013, 2005a.

Chiarabba, C., De Gori, P., Chiaraluce, L., Bordoni, P., Cattaneo, M., De Martin, M., Frepoli, A., Michelini, A., Monachesi, A., Moretti, M., Augliera, G. P., D'Alema, E., Frapiccini, M., Gassi, A., Marzorati, S., Bartolomeo, P. D., Gentile, S., Govoni, A., Lovisa, L., Romanelli, M., Ferretti, G., Pasta, M., Spallarossa, D., and Zunino, E.: Mainshocks and aftershocks of the 2002 molise seismic sequence, southern Italy, J Seismol, 9, 487–494, https://doi.org/10.1007/s10950-005-0633-9, 2005b.

Chiarabba, C., Bagh, S., Bianchi, I., De Gori, P., and Barchi, M.: Deep structural heterogeneities and the tectonic evolution of the Abruzzi region (Central Apennines, Italy) revealed by microseismicity, seismic tomography, and teleseismic receiver functions, Earth and Planetary Science Letters, 295, 462–476, https://doi.org/10.1016/j.epsl.2010.04.028, 2010.

Chiarabba, C., Buttinelli, M., Cattaneo, M., and De Gori, P.: Large Earthquakes Driven by Fluid Overpressure: The Apennines Normal Faulting System Case, Tectonics, 39, https://doi.org/10.1029/2019TC006014, 2020.

Cimini, G. B. and De Gori, P.: Nonlinear *P* -wave tomography of subducted lithosphere beneath central-southern Apennines (Italy), Geophys. Res. Lett., 28, 4387–4390, https://doi.org/10.1029/2001GL013546, 2001.

Custódio, S., Dias, N. A., Carrilho, F., Góngora, E., Rio, I., Marreiros, C., Morais, I., Alves, P., and Matias, L.: Earthquakes in western Iberia: improving the understanding of lithospheric deformation in a slowly deforming region, Geophys. J. Int., 203, 127–145, https://doi.org/10.1093/gji/ggv285, 2015.

D'Ambrosio, A., Lipparini, L., Bigi, S., Cassola, T., Bambridge, V. R., Derks, J. F., and Trippetta, F.: Structural restoration and basin modelling of the central apennine orogen/foredeep/foreland system: New insights on the regional petroleum system, Marine and Petroleum Geology, 127, 104948, https://doi.org/10.1016/j.marpetgeo.2021.104948, 2021.

Delaunay, B.: Sur la sphere vide, Izv. Akad. Nauk SSSR, Otdelenie Matematicheskii i Estestvennyka Nauk, 7, 1–2, 1934.

Devoti, R., D'Agostino, N., Serpelloni, E., Pietrantonio, G., Riguzzi, F., Avallone, A., Cavaliere, A., Cheloni, D., Cecere, G., D'Ambrosio, C., Franco, L., Selvaggi, G., Metois, M., Esposito, A., Sepe, V., Galvani, A., and Anzidei, M.: A Combined Velocity Field of the Mediterranean Region, Annals of Geophysics, 60, 1, https://doi.org/10.4401/ag-7059, 2017.

Di Luccio, F., Fukuyama, E., and Pino, N. A.: The 2002 Molise earthquake sequence: What can we learn about the tectonics of southern Italy?, Tectonophysics, 405, 141–154, https://doi.org/10.1016/j.tecto.2005.05.024, 2005.

Di Luzio, E., Mele, G., Tiberti, M. M., Cavinato, G. P., and Parotto, M.: Moho deepening and shallow upper crustal delamination beneath the central Apennines, Earth and Planetary Science Letters, 280, 1–12, https://doi.org/10.1016/j.epsl.2008.09.018, 2009.

Di Stefano, R., Bianchi, I., Ciaccio, M. G., Carrara, G., and Kissling, E.: Three-dimensional Moho topography in Italy: New constraints from receiver functions and controlled source seismology: NEW MOHO MAP OF ITALY, Geochem. Geophys. Geosyst., 12, n/a-n/a, https://doi.org/10.1029/2011GC003649, 2011.

DISS Working Group: Database of Individual Seismogenic Sources (DISS), version 3.3.0: A compilation of potential sources for earthquakes larger than M 5.5 in Italy and surrounding areas., 132 Individual Seismogenic Sources, 197 Composite Seismogenic Sources, 38 Debated Seismogenic Sources, 4 Subduction Zones, https://doi.org/10.13127/DISS3.3.0, 2021.

Doglioni, C.: Tectonics of the Dolomites (southern alps, northern Italy), Journal of Structural Geology, 9, 181–193, https://doi.org/10.1016/0191-8141(87)90024-1, 1987.

Ferrarini, F., Lavecchia, G., De Nardis, R., and Brozzetti, F.: Fault Geometry and Active Stress from Earthquakes and Field Geology Data Analysis: The Colfiorito 1997 and L'Aquila 2009 Cases (Central Italy), Pure Appl. Geophys., 172, 1079–1103, https://doi.org/10.1007/s00024-014-0931-7, 2015.

Ferrarini, F., Boncio, P., de Nardis, R., Pappone, G., Cesarano, M., Aucelli, P. P. C., and Lavecchia, G.: Segmentation pattern and structural complexities in seismogenic extensional settings: The North Matese Fault System (Central Italy), Journal of Structural Geology, 95, 93–112, https://doi.org/10.1016/j.jsg.2016.11.006, 2017.

Ferrarini, F., Arrowsmith, J. R., Brozzetti, F., de Nardis, R., Cirillo, D., Whipple, K. X., and Lavecchia, G.: Late Quaternary Tectonics along the Peri-Adriatic Sector of the Apenninic Chain (Central-Southern Italy): Inspecting Active Shortening through Topographic Relief and Fluvial Network Analyses, Litosphere, 2021, https://doi.org/10.2113/2021/7866617, 2021a.

Ferrarini, F., de Nardis, R., Brozzetti, F., Cirillo, D., Arrowsmith, J. R., and Lavecchia, G.: Multiple Lines of Evidence for a Potentially Seismogenic Fault Along the Central-Apennine (Italy) Active Extensional Belt–An Unexpected Outcome of the MW6.5 Norcia 2016 Earthquake, Front. Earth Sci., 9, 642243, https://doi.org/10.3389/feart.2021.642243, 2021b.

Fracassi, U. and Valensise, G.: Unveiling the Sources of the Catastrophic 1456 Multiple Earthquake: Hints to an Unexplored Tectonic Mechanism in Southern Italy, Bulletin of the Seismological Society of America, 97, 725–748, https://doi.org/10.1785/0120050250, 2007.

Frepoli, A., Cimini, G. B., De Gori, P., De Luca, G., Marchetti, A., Monna, S., Montuori, C., and Pagliuca, N. M.: Seismic sequences and swarms in the Latium-Abruzzo-Molise Apennines (central Italy): New observations and analysis from a dense monitoring of the recent activity, Tectonophysics, 712–713, 312–329, https://doi.org/10.1016/j.tecto.2017.05.026, 2017.

Galadini, F. and Galli, P.: Active Tectonics in the Central Apennines (Italy) – Input Data for Seismic Hazard Assessment, 2000.

Galli, P. and Pallone, F.: Reviewing the intensity distribution of the 1933 earthquake (Maiella, central Italy). Clues on the seismogenic fault, AMQ, 32, 93–100, https://doi.org/10.26382/AMQ.2019.05, 2019.

Galli, P., Giaccio, B., Peronace, E., and Messina, P.: Holocene Paleoearthquakes and Early–Late Pleistocene Slip Rate on the Sulmona Fault (Central Apeninnes, Italy), Bulletin of the Seismological Society of America, 105, 1–13, https://doi.org/10.1785/0120140029, 2015.

Ghisetti, F. and Vezzani, L.: Normal faulting, transcrustal permeability and seismogenesis in the Apennines (Italy), Tectonophysics, 348, 155–168, https://doi.org/10.1016/S0040-1951(01)00254-2, 2002.

Ghisetti, F., Barchi, M., Bally, A. W., Moretti, I., and Vezzani, L.: Conflicting Balanced Structural Sections Across the Central Apennines (Italy): Problems and Implications, in: Generation, Accumulation and Production of Europe's Hydrocarbons III, edited by: Spencer, A. M., Springer Berlin Heidelberg, Berlin, Heidelberg, 219–231, https://doi.org/10.1007/978-3-642-77859-9_18, 1993.

Giacomuzzi, G., De Gori, P., and Chiarabba, C.: How mantle heterogeneities drive continental subduction and magmatism in the Apennines, Sci Rep, 12, 13631, https://doi.org/10.1038/s41598-022-17715-w, 2022.

Gómez-Novell, O., García-Mayordomo, J., Ortuño, M., Masana, E., and Chartier, T.: Fault System-Based Probabilistic Seismic Hazard Assessment of a Moderate Seismicity Region: The Eastern Betics Shear Zone (SE Spain), Front. Earth Sci., 8, 579398, https://doi.org/10.3389/feart.2020.579398, 2020.

Govoni, A., Marchetti, A., De Gori, P., Di Bona, M., Lucente, F. P., Improta, L., Chiarabba, C., Nardi, A., Margheriti, L., Agostinetti, N. P., Di Giovambattista, R., Latorre, D., Anselmi, M., Ciaccio, M. G., Moretti, M., Castellano, C., and Piccinini, D.: The 2012 Emilia seismic sequence (Northern Italy): Imaging the thrust fault system by accurate aftershock location, Tectonophysics, 622, 44–55, https://doi.org/10.1016/j.tecto.2014.02.013, 2014.

Guidoboni, E., Ferrari, G., Mariotti, D., Comastri, A., Tarabusi, G., Sgattoni, G., and Valensise, G.: CFTI5Med, Catalogo dei Forti Terremoti in Italia (461 a.C.-1997) e nell'area Mediterranea (760 a.C.-1500), https://doi.org/10.6092/INGV.IT-CFTI5, 1 April 2018.

Guidoboni, E., Ferrari, G., Tarabusi, G., Sgattoni, G., Comastri, A., Mariotti, D., Ciuccarelli, C., Bianchi, M. G., and Valensise, G.: CFTI5Med, the new release of the catalogue of strong earthquakes in Italy and in the Mediterranean area, Sci Data, 6, 80, https://doi.org/10.1038/s41597-019-0091-9, 2019.

Improta, L., De Gori, P., and Chiarabba, C.: New insights into crustal structure, Cenozoic magmatism, CO_2 degassing, and seismogenesis in the southern Apennines and Irpinia region from local earthquake tomography: seismic tomography of Apennines, J. Geophys. Res. Solid Earth, 119, 8283–8311, https://doi.org/10.1002/2013JB010890, 2014.

Improta, L., Cirella, A., Pezzo, G., Molinari, I., and Piatanesi, A.: Joint Inversion of Geodetic and Strong Motion Data for the 2012, M_w 6.1–6.0, May 20th and May 29th, Northern Italy Earthquakes: Source Models and Seismotectonic Interpretation, JGR Solid Earth, 128, e2022JB026278, https://doi.org/10.1029/2022JB026278, 2023.

International Seismological Center: ISC online Bulletin, https://doi.org/10.31905/D808B830, 2024.

ISIDe Working Group: Italian Seismological Instrumental and Parametric Database (ISIDe), https://doi.org/10.13127/ISIDE, 2007.

Kirby, E., Whipple, K., and Harkins, N.: Topography reveals seismic hazard, Nature Geosci, 1, 485–487, https://doi.org/10.1038/ngeo265, 2008.

Lacombe, O. and Bellahsen, N.: Thick-skinned tectonics and basement-involved fold–thrust belts: insights from selected Cenozoic orogens, Geol. Mag., 153, 763–810, https://doi.org/10.1017/S0016756816000078, 2016.

Lanari, R., Reitano, R., Faccenna, C., Agostinetti, N. P., and Ballato, P.: Surface and Crustal Response to Deep Subduction Dynamics: Insights From the Apennines, Italy, Tectonics, 42, e2022TC007461, https://doi.org/10.1029/2022TC007461, 2023.

Latorre, D., Di Stefano, R., Castello, B., Michele, M., and Chiaraluce, L.: An updated view of the Italian seismicity from probabilistic location in 3D velocity models: The 1981–2018 Italian catalog of absolute earthquake locations (CLASS), Tectonophysics, 846, 229664, https://doi.org/10.1016/j.tecto.2022.229664, 2023.

Lavecchia, G. and Creati, N.: A mantle plume head trapped in the transition zone beneath the Mediterranean: a new idea, Ann. Geoph., 49, 2006.

Lavecchia, G., Brozzetti, F., Barchi, M., Menichetti, M., and Keller, J. V. A.: Seismotectonic zoning in east-central Italy deduced from an analysis of the Neogene to present deformations and related stress fields, Geological Society of America Bulletin, 106, 1107–1120, https://doi.org/10.1130/0016-7606(1994)106<1107:SZIECI>2.3.CO;2, 1994.

Lavecchia, G., Nardis, R. D., Visini, F., Ferrarini, F., and Barbano, M. S.: Seismogenic evidence of ongoing compression in eastern-central Italy and mainland Sicily: a comparison, Boll. Soc. Geol. It., 126, 209–222, 2007.

Lavecchia, G., De Nardis, R., Costa, G., Tiberi, L., Ferrarini, F., Cirillo, D., Brozzetti, F., and Suhadolc, P.: Was the Mirandola Thrust Really Involved in the Emilia 2012 Seismic Sequence (northern Italy)? Implications on the likelihood of triggered seismicity effects, BGTA, https://doi.org/10.4430/bgta0162, 2015.

Lavecchia, G., Adinolfi, G. M., De Nardis, R., Ferrarini, F., Cirillo, D., Brozzetti, F., De Matteis, R., Festa, G., and Zollo, A.: Multidisciplinary inferences on a newly recognized active east-dipping extensional system in Central Italy, Terra Nova, 29, 77–89, https://doi.org/10.1111/ter.12251, 2017.

Lavecchia, G., Bello, S., Andrenacci, C., Cirillo, D., Ferrarini, F., Vicentini, N., de Nardis, R., and Brozzetti, F.: Host Faults Database of central Italy, https://doi.org/10.5281/ZENODO.6412501, 2021a.

Lavecchia, G., De Nardis, R., Ferrarini, F., Cirillo, D., Bello, S., and Brozzetti, F.: Regional Seismotectonic Zonation of Hydrocarbon Fields in Active Thrust Belts: A Case Study from Italy, in: Building Knowledge for Geohazard Assessment and Management in the Caucasus and other Orogenic Regions, edited by: Bonali, F. L., Pasquaré Mariotto, F., and Tsereteli, N., Springer Netherlands, Dordrecht, 89–128, https://doi.org/10.1007/978-94-024-2046-3_7, 2021b.

Lavecchia, G., Bello, S., Andrenacci, C., Cirillo, D., Ferrarini, F., Vicentini, N., De Nardis, R., Roberts, G., and Brozzetti, F.: QUaternary fault strain INdicators database - QUIN 1.0 - first release from the Apennines of central Italy, Sci Data, 9, 204, https://doi.org/10.1038/s41597-022-01311-8, 2022.

Lavecchia, G., Bello, S., Cirillo, D., Pietrolungo, F., and Brozzetti, F.: Quaternary-Host Faults Database 2.0 (Southern Italy), https://doi.org/10.5281/ZENODO.8414479, 2023a.

Lavecchia, G., Pietrolungo, F., Bello, S., Talone, D., Pandolfi, C., Andrenacci, C., Carducci, A., and De Nardis, R.: Slowly Deforming Megathrusts within the Continental Lithosphere: A Case from Italy, GSAT, 4, https://doi.org/10.1130/GSATG573A.1, 2023b.

Lavecchia, G., Brozzetti, F., Bello, S., and De Nardis, R.: Mapping fault architecture from depth to surface: integrating microseismicity and structural geology in low-strain Apennine regions, Journal of Structural Geology, 105518, https://doi.org/10.1016/j.jsg.2025.105518, 2025.

Lu, Y., Wetzler, N., Waldmann, N., Agnon, A., Biasi, G. P., and Marco, S.: A 220,000-year-long continuous large earthquake record on a slow-slipping plate boundary, Sci. Adv., 6, eaba4170, https://doi.org/10.1126/sciadv.aba4170, 2020.

Mariucci, M. T. and Montone, P.: IPSI 1.5, Italian Present-day Stress Indicators Dataset, https://doi.org/10.13127/IPSI.1.5, 2022.

Martín-Banda, R., Insua-Arévalo, J. M., and García-Mayordomo, J.: Slip Rate Variation During the Last ~210 ka on a Slow Fault in a Transpressive Regime: The Carrascoy Fault (Eastern Betic Shear Zone, SE Spain), Front. Earth Sci., 8, 599608, https://doi.org/10.3389/feart.2020.599608, 2021.

Matos, C., Custódio, S., Batló, J., Zahradník, J., Arroucau, P., Silveira, G., and Heimann, S.: An Active Seismic Zone in Intraplate West Iberia Inferred From High-Resolution Geophysical Data, JGR Solid Earth, 123, 2885–2907, https://doi.org/10.1002/2017JB015114, 2018.

Mazzoli, S., Corrado, S., De Donatis, M., Scrocca, D., Butler, R. W. H., Di Bucci, D., Naso, G., Nicolai, C., and Zucconi, V.: Time and space variability of «thin-skinned » and «thick-skinned » thrust tectonics in the Apennines (Italy), Rend. Fis. Acc. Lincei, 11, 5–39, 2000.

Mazzotti, A. P., Stucchi, E., Fradelizio, G. L., Zanzi, L., and Scandone, P.: Seismic exploration in complex terrains: A processing experience in the Southern Apennines, GEOPHYSICS, 65, 1402–1417, https://doi.org/10.1190/1.1444830, 2000.

Mazzotti, S., Jomard, H., and Masson, F.: Processes and deformation rates generating seismicity in metropolitan France and conterminous Western Europe, BSGF - Earth Sci. Bull., 191, 19, https://doi.org/10.1051/bsgf/2020019, 2020.

Miccolis, S., Filippucci, M., De Lorenzo, S., Frepoli, A., Pierri, P., and Tallarico, A.: Seismogenic Structure Orientation and Stress Field of the Gargano Promontory (Southern Italy) From Microseismicity Analysis, Front. Earth Sci., 9, 589332, https://doi.org/10.3389/feart.2021.589332, 2021.

Michele, M., Latorre, D., and Emolo, A.: An Empirical Formula to Classify the Quality of Earthquake Locations, Bulletin of the Seismological Society of America, 109, 2755–2761, https://doi.org/10.1785/0120190144, 2019.

Milano, G., Di Giovambattista, R., and Ventura, G.: Seismic constraints on the present-day kinematics of the Gargano foreland, Italy, at the transition zone between the southern and northern Apennine belts, Geophys. Res. Lett., 32, L24308, https://doi.org/10.1029/2005GL024604, 2005.

Milano, P.: Present-day seismicity of the Matese Massif (central-southern Apennines, Italy):new constraints on the seismotectonic setting of the central and southern sides, BGO, https://doi.org/10.4430/bgo00414, 2023.

Montone, P. and Mariucci, M. T.: Deep well new data in the area of the 2022 Mw 5.5 earthquake, Adriatic Sea, Italy: In situ stress state and P-velocities, Front. Earth Sci., 11, 1164929, https://doi.org/10.3389/feart.2023.1164929, 2023.

Mostardini, F. and Merlini, S.: Appennino Centro Meridionale - Sezioni Geologiche e Proposta di Modello Strutturale, Mem. Soc. Geol. It., 177–202, 1986.

de Nardis, R.: A Temporary Seismic Monitoring of the Sulmona Area (Abruzzo,Italy) for Seismotectonic Purposes, BGTA, https://doi.org/10.4430/bgta0026, 2011.

de Nardis, R., Pace, B., Lavecchia, G., Visini, F., and Boncio, P.: Geological and Macroseismic Data For Seismotectonic Purpose: The 1706 Maiella (Abruzzo, Italy) Earthquake Case Study, AGU Fall Meeting Abstracts, 1, 1946, 2008.

de Nardis, R., Pandolfi, C., Cattaneo, M., Monachesi, G., Cirillo, D., Ferrarini, F., Bello, S., Brozzetti, F., and Lavecchia, G.: Lithospheric double shear zone unveiled by microseismicity in a region of slow deformation, Sci Rep, 12, 21066, https://doi.org/10.1038/s41598-022-24903-1, 2022.

de Nardis, R., Vuan, A., Carbone, L., Talone, D., Romano, M. A., and Lavecchia, G.: Interplay of tectonic and dynamic processes shaping multilayer extensional system in southern-central Apennines, Sci Rep, 14, 18375, https://doi.org/10.1038/s41598-024-69118-8, 2024.

Nicholson, C., Plesch, A., Sorlien, C. C., Shaw, J. H., and Hauksson, E.: The SCEC 3D community fault model (CFM-v5): An updated and expanded fault set of oblique crustal deformation and complex fault interaction for southern California, in: AGU Fall Meeting Abstracts, T31B-4584, 2014.

Noguera, A. M. and Rea, G.: Deep structure of the Campanian–Lucanian Arc (Southern Apennine, Italy), Tectonophysics, 324, 239–265, https://doi.org/10.1016/S0040-1951(00)00137-2, 2000.

Okabe, A., Boots, B., Sugihara, K., and Chiu, S. N.: Spatial tessellations: concepts and applications of Voronoi diagrams, 1992.

Onana, P. N. E., Toto, E. A., Zouhri, L., Chaabane, A., El Mouraouah, A., and Iben Brahim, A.: Recent seismicity of Central High Atlas and Ouarzazate basin (Morocco), Bull Eng Geol Environ, 70, 633–641, https://doi.org/10.1007/s10064-011-0361-z, 2011.

Orecchio, B., Scolaro, S., Batlló, J., Neri, G., Presti, D., Stich, D., and Totaro, C.: New Results for the 1968 Belice, South Italy, Seismic Sequence: Solving the Long-Lasting Ambiguity on Causative Source, Seismological Research Letters, 92, 2364–2381, https://doi.org/10.1785/0220200277, 2021.

Pace, B., Peruzza, L., Lavecchia, G., and Boncio, P.: Layered Seismogenic Source Model and Probabilistic Seismic-Hazard Analyses in Central Italy, Bulletin of the Seismological Society of America, 96, 1567, https://doi.org/10.1785/0120060050, 2006.

Pandolfi, C., Taroni, M., De Nardis, R., Lavecchia, G., and Akinci, A.: Combining Seismotectonic and Catalog-Based 3D Models for Advanced Smoothed Seismicity Computations, Seismological Research Letters, 95, 10–20, https://doi.org/10.1785/0220230088, 2023.

Pandolfi, C., Taroni, M., De Nardis, R., Lavecchia, G., and Akinci, A.: Advanced 3D seismic hazard analysis for active compression in the Adriatic Thrust Zone, Italy, Bull Earthquake Eng, https://doi.org/10.1007/s10518-024-01948-3, 2024.

Patacca, E. and Scandone, P.: THE PLIO-PLEISTOCENE THRUST BELT - FOREDEEP SYSTEM IN THE SOUTHERN APENNINES AND SICILY (ITALY), Special Volume of the Italian Geological Society for the IGC, 2004.

Patacca, E., Scandone, P., Di Luzio, E., Cavinato, G. P., and Parotto, M.: Structural architecture of the central Apennines: Interpretation of the CROP 11 seismic profile from the Adriatic coast to the orographic divide: CROP 11 SEISMIC PROFILE, Tectonics, 27, n/a-n/a, https://doi.org/10.1029/2005TC001917, 2008.

Petricca, P., Carminati, E., and Doglioni, C.: The Decollement Depth of Active Thrust Faults in Italy: Implications on Potential Earthquake Magnitude, Tectonics, 38, 3990–4009, https://doi.org/10.1029/2019TC005641, 2019.

Pezzo, G., Petracchini, L., Devoti, R., Maffucci, R., Anderlini, L., Antoncecchi, I., Billi, A., Carminati, E., Ciccone, F., Cuffaro, M., Livani, M., Palano, M., Petricca, P., Pietrantonio, G., Riguzzi, F., Rossi, G., Sparacino, F., and Doglioni, C.:

Active Fold-Thrust Belt to Foreland Transition in Northern Adria, Italy, Tracked by Seismic Reflection Profiles and GPS Offshore Data, Tectonics, 39, https://doi.org/10.1029/2020TC006425, 2020.

Piccinini, D., Chiarabba, C., Augliera, P., and Monghidoro Earthquake Group (M.E.G.): Compression along the northern Apennines? Evidence from the Mw 5.3 Monghidoro earthquake, Terra Nova, 18, 89–94, https://doi.org/10.1111/j.1365-3121.2005.00667.x, 2006.

Plesch, A., Shaw, J. H., Benson, C., Bryant, W. A., Carena, S., Cooke, M., Dolan, J., Fuis, G., Gath, E., Grant, L., Hauksson, E., Jordan, T., Kamerling, M., Legg, M., Lindvall, S., Magistrale, H., Nicholson, C., Niemi, N., Oskin, M., Perry, S., Planansky, G., Rockwell, T., Shearer, P., Sorlien, C., Suss, M. P., Suppe, J., Treiman, J., and Yeats, R.: Community Fault Model (CFM) for Southern California, Bulletin of the Seismological Society of America, 97, 1793–1802, https://doi.org/10.1785/0120050211, 2007.

Pomposo, G. and Pizzi, A.: Evidence of recent and active tectonics in the buried external sector of the Abruzzi central Appennines; [Evidenze di tettonica recente ed attiva nel settore esterno sepolto dell'Appennino centrale abruzzese], Rendiconti Online Societa Geologica Italiana, 5, 176–178, 2009.

Pondrelli, S., Salimbeni, S., Ekström, G., Morelli, A., Gasperini, P., and Vannucci, G.: The Italian CMT dataset from 1977 to the present, Physics of the Earth and Planetary Interiors, 159, 286–303, https://doi.org/10.1016/j.pepi.2006.07.008, 2006.

Puliti, I., Pizzi, A., Gori, S., Falcucci, E., Galadini, F., Moro, M., and Saroli, M.: Paleoseismological evidence of multiple, large-magnitude earthquake surface ruptures on the active Mt. Morrone normal fault, central Apennines, Italy, Solid Earth, 16, 275–296, https://doi.org/10.5194/se-16-275-2025, 2025.

Racano, S., Fubelli, G., Centamore, E., Bonasera, M., and Dramis, F.: Geomorphological detection of surface effects induced by active blind thrusts in the southern Abruzzi peri-Adriatic belt (Central Italy), Geografia Fisica e Dinamica Quaternaria, 3–13, https://doi.org/10.4461/GFDQ.2020.43.1, 2020.

Ramalho, M., Matias, L., Neres, M., Carafa, M. M. C., Carvalho, A., and Teves-Costa, P.: A sanity check for earthquake recurrence models used in PSHA of slowly deforming regions: the case of SW Iberia, Nat. Hazards Earth Syst. Sci., 22, 117–138, https://doi.org/10.5194/nhess-22-117-2022, 2022.

Rawlinson, N. and Spakman, W.: On the use of sensitivity tests in seismic tomography, Geophys. J. Int., 205, 1221–1243, https://doi.org/10.1093/gji/ggw084, 2016

Rawlinson, N. and Sambridge, M.: Seismic wavefront tracking in 3D heterogeneous media: applications with multiple data classes, Explt. Geophys., 37, 9, 2006.

Rawlinson, N. and Urvoy, M.: Simultaneous inversion of active and passive source datasets for 3-D seismic structure with application to Tasmania, Geophys. Res. Lett., 33, L24313, https://doi.org/10.1029/2006GL028105, 2006.

Reasenberg, P. and Oppenheimer, D.: FPFIT, FPPLOT and FPPAGE: FORTRAN computer programs for calculating and displaying earthquake fault-plane solution, U.S. Geological Survey, Open-File Report, 85–739, 1985.

Romano, M. A., de Nardis, R., Lavecchia, G., Garbin, M., Peruzza, L., Priolo, E., Romanelli, M., and Ferrarini, F.: Preliminary analysis of the microearthquakes-faults association in the Sulmona basin (central Apennines, Italy), Rend. Online Soc. Geol. It., 29, 150–153, 2013a.

Romano, M. A., De Nardis, R., Garbin, M., Peruzza, L., Priolo, E., Lavecchia, G., and Romanelli, M.: Temporary seismic monitoring of the Sulmona area (Abruzzo, Italy): a quality study of microearthquake locations, Nat. Hazards Earth Syst. Sci., 13, 2727–2744, https://doi.org/10.5194/nhess-13-2727-2013, 2013b.

Rovida, A., Locati, M., Camassi, R., Lolli, B., and Gasperini, P.: The Italian earthquake catalogue CPTI15, Bulletin of Earthquake Engineering, 18, 2953–2984, https://doi.org/10.1007/s10518-020-00818-y, 2020.

Rovida, A., Locati, M., Camassi, R., Lolli, B., Gasperini, P., and Antonucci, A.: Catalogo Parametrico dei Terremoti Italiani (CPTI15), versione 4.0 (4.0), https://doi.org/10.13127/CPTI/CPTI15.4, 2022.

Scafidi, D., Solarino, S., and Eva, C.: P wave seismic velocity and Vp/Vs ratio beneath the Italian peninsula from local earthquake tomography, Tectonophysics, 465, 1–23, https://doi.org/10.1016/j.tecto.2008.07.013, 2009.

Schorlemmer, D., Mele, F., and Marzocchi, W.: A completeness analysis of the National Seismic Network of Italy, J. Geophys. Res., 115, B04308, https://doi.org/10.1029/2008JB006097, 2010.

Scognamiglio, L., Tinti, E., and Quintiliani, M.: Time Domain Moment Tensor (TDMT) - ISTITUTO NAZIONALE DI GEOFISICA E VULCANOLOGIA, https://doi.org/10.13127/tdmt, 2006.

Scrocca, D., Carminati, E., and Doglioni, C.: Deep structure of the southern Apennines, Italy: Thin-skinned or thick-skinned?: DEEP STRUCTURE OF THE SOUTHERN APENNINES, Tectonics, 24, n/a-n/a, https://doi.org/10.1029/2004TC001634, 2005.

Sébrier, M., Siame, L., Zouine, E. M., Winter, T., Missenard, Y., and Leturmy, P.: Active tectonics in the Moroccan High Atlas, Comptes Rendus. Géoscience, 338, 65–79, https://doi.org/10.1016/j.crte.2005.12.001, 2006.

Speranza, F. and Chiappini, M.: Thick-skinned tectonics in the external Apennines, Italy: New evidence from magnetic anomaly analysis: THICK-SKINNED TECTONICS IN THE APENNINES, J. Geophys. Res., 107, ETG 8-1-ETG 8-19, https://doi.org/10.1029/2000JB000027, 2002.

Steckler, M. S., Agostinetti, N. P., Wilson, C. K., Roselli, P., Seeber, L., Amato, A., and Lerner-Lam, A.: Crustal structure in the Southern Apennines from teleseismic receiver functions, Geol, 36, 155, https://doi.org/10.1130/G24065A.1, 2008.

Talone, D., De Siena, L., Lavecchia, G., and De Nardis, R.: The Attenuation and Scattering Signature of Fluid Reservoirs and Tectonic Interactions in the Central-Southern Apennines (Italy), Geophys. Res. Lett., https://doi.org/10.1029/2023GL106074, 2023.

Taroni, M. and Carafa, M. M. C.: Earthquake size distributions are slightly different in compression vs extension, Commun Earth Environ, 4, 398, https://doi.org/10.1038/s43247-023-01059-y, 2023.

Tibaldi, A., De Nardis, R., Torrese, P., Bressan, S., Pedicini, M., Talone, D., Bonali, F. L., Corti, N., Russo, E., and Lavecchia, G.: A multi-scale approach to the recent activity of the Stradella thrust in the seismotectonic context of the Emilia Arc (northwestern Italy), Tectonophysics, 857, 229853, https://doi.org/10.1016/j.tecto.2023.229853, 2023.

Tozer, R. S. J., Butler, R. W. H., and Corrado, S.: Comparing thin- and thick-skinned thrust tectonic models of the Central Apennines, Italy, Stephan Mueller Spec. Publ. Ser., 1, 181–194, https://doi.org/10.5194/smsps-1-181-2002, 2002.

Trionfera, B., Frepoli, A., De Luca, G., De Gori, P., and Doglioni, C.: The 2013–2018 Matese and Beneventano Seismic Sequences (Central–Southern Apennines): New Constraints on the Hypocentral Depth Determination, Geosciences, 10, 17, https://doi.org/10.3390/geosciences10010017, 2019.

Trippetta, F., Durante, D., Lipparini, L., Romi, A., and Brandano, M.: Carbonate-ramp reservoirs modelling best solutions: Insights from a dense shallow well database in Central Italy, Marine and Petroleum Geology, 126, 104931, https://doi.org/10.1016/j.marpetgeo.2021.104931, 2021.

Turrini, C., Lacombe, O., and Roure, F.: Present-day 3D structural model of the Po Valley basin, Northern Italy, Marine and Petroleum Geology, 56, 266–289, https://doi.org/10.1016/j.marpetgeo.2014.02.006, 2014.

Van Der Wal, J. L. N., Nottebaum, V. C., Stauch, G., Binnie, S. A., Batkhishig, O., Lehmkuhl, F., and Reicherter, K.: Geomorphological Evidence of Active Faulting in Low Seismicity Regions—Examples From the Valley of Gobi Lakes, Southern Mongolia, Front. Earth Sci., 8, 589814, https://doi.org/10.3389/feart.2020.589814, 2021.

Vannoli, P., Burrato, P., and Valensise, G.: The Seismotectonics of the Po Plain (Northern Italy): Tectonic Diversity in a Blind Faulting Domain, Pure Appl. Geophys., 172, 1105–1142, https://doi.org/10.1007/s00024-014-0873-0, 2015.

Vezzani, L., Festa, A., and Ghisetti, F. C.: Geology and Tectonic Evolution of the Central-Southern Apennines, Italy, Geol. Soc. Am., 2010.

Visini, F., Nardis, R. D., Barbano, M. S., and Lavecchia, G.: Testing the seismogenic sources of the January 11th 1693 Sicilian earthquake (Io X/XI): insights from macroseismic field simulations, Ital.J.Geosci., 128, 147–156, 2009.

Visini, F., De Nardis, R., and Lavecchia, G.: Rates of active compressional deformation in central Italy and Sicily: evaluation of the seismic budget, Int J Earth Sci (Geol Rundsch), 99, 243–264, https://doi.org/10.1007/s00531-009-0473-x, 2010.

Volatili, T., Gironelli, V., Luzi, L., Galli, P., Carafa, M. M. C., and Tondi, E.: Elusive seismogenic sources of historical earthquakes: insights from the Mw 6.8, 1706 Maiella earthquake (central Italy), Bull Earthquake Eng, 23, 1279–1296, https://doi.org/10.1007/s10518-025-02110-3, 2025.

Wortel, M. J. R. and Spakman, W.: Subduction and Slab Detachment in the Mediterranean-Carpathian Region, Science, 290, 1910–1917, https://doi.org/10.1126/science.290.5498.1910, 2000.

Yeck, W. L., Hatem, A. E., Goldberg, D. E., Barnhart, W. D., Jobe, J. A. T., Shelly, D. R., Villaseñor, A., Benz, H. M., and Earle, P. S.: Rapid Source Characterization of the 2023 Mw 6.8 Al Haouz, Morocco, Earthquake, The Seismic Record, 3, 357–366, https://doi.org/10.1785/0320230040, 2023.

Zhang, Y., Feng, W., Xu, L., Zhou, C., and Chen, Y.: Spatio-temporal rupture process of the 2008 great Wenchuan earthquake, Sci. China Ser. D-Earth Sci., 52, 145–154, https://doi.org/10.1007/s11430-008-0148-7, 2009.

Zhao, L., Paul, A., Malusà, M. G., Xu, X., Zheng, T., Solarino, S., Guillot, S., Schwartz, S., Dumont, T., Salimbeni, S., Aubert, C., Pondrelli, S., Wang, Q., and Zhu, R.: Continuity of the Alpine slab unraveled by high-resolution *P* wave tomography: Continuity of the Alpine Slab, J. Geophys. Res. Solid Earth, 121, 8720–8737, https://doi.org/10.1002/2016JB013310, 2016.